



RIVAS
SCP0-GA-2010-265754



RIVAS
Railway Induced Vibration Abatement Solutions
Collaborative project

Validation of wheel maintenance measures on the rolling stock for reduced excitation of ground vibration

Deliverable D2.9

Submission date: 31/12/2013

Project Coordinator:

Wolfgang Behr

International Union of Railways (UIC)

ext.behr@uic.org

Title	Validation of wheel maintenance measures on the rolling stock for reduced excitation of ground vibration
Domain	WP 2
Date	31.12.2013
Author/Authors	Roger Müller, Daniel Leibundgut, Bert Stallaert, Lise Pesqueux, Alf Ekblad
Partner	SBB, D2S, Alstom, Trafikverket
Document Code	RIVAS_SBB_WP2_D2_9_V5
Version	5
Status	Final

Dissemination level:

Project co-funded by the European Commission within the Seventh Framework Programme		
Dissemination Level		
PU	Public	X
PP	Restricted to other programme participants (including the Commission Services)	
RE	Restricted to a group specified by the consortium (including the Commission) Services)	
CO	Confidential, only for members of the consortium (including the Commission Services)	

Document history		
Revision	Date	Description
1	06/11/2013	Skeleton report
2	04/12/2013	First draft
3	15/12/2013	Second draft
4	18/12/2013	Final draft
5	31/12/2013	Final

1. EXECUTIVE SUMMARY

In the frame of the EU FP7 project 'Railway induced vibration abatement solutions (RIVAS)', abatement measures for mitigating ground-borne noise and vibrations through wheel and track maintenance were studied.

The final step in the project, described in the current report, consisted of measurement campaigns designed to quantify the influence of rolling stock maintenance on ground-borne vibrations. A short term measurement campaign was performed with a dedicated test train (front and tail locomotive), composed to have a sufficient spread in wheel-out-of-roundness among the different wagons which can be seen in the vibration pass-by measurements. Both the wheel and rail irregularities were determined by direct measurements of the wheel and rail vertical profile. Out-of-roundness measurements show high levels of wheel defects on a locomotive already a few weeks after wheel reprofiling. These test train tests took place in Dottikon and Brunnen in Switzerland where the test train was run several times at different speeds.

A second measurement campaign used a measurement station in Brunnen in Switzerland to perform long term vibration measurements with the purpose of validating wheel maintenance mitigation measures.

It could be observed for the test train measurements both in Dottikon and in Brunnen that a reduction of the wheel irregularities with the amount of X dB by removing wheel out-of-roundness by maintenance roughly reduces the ground vibration with around an amount of X dB. This can be seen in the test train measurements of vibration and wheel out-of-roundness: both show differences of up to 20 dB between newly maintained and worn wheels of the locomotives. Dynamic force measurements also show similar amplitude differences.

In addition, the comparison of older OOR measurements with actual vibration measurements of the long term measurement campaign in Brunnen show similar amplitudes in some frequency bands. The vibration level scattering (95%-median value) for different vehicle types shows potential for improvement by maintenance. The insertion loss for some of the Re420 freight locomotives could reach values up to 12 dB. For Intercity trains, which are maintained more regularly to reduce structure borne noise in the vehicle, the potential for vibration reduction is low. The vibration spread for CARGO wagons is similar to the Locomotive Re420 and indicates potential for maintenance.

A statistical reanalysis of vibration measurements at different sites in Switzerland (Thun, Ligerz and Cadenazzo) indicate respectable potential for some of the vehicle types to reduce vibration excitation by maintenance. The freight wagons with bogie Y25 show for all 3 sites more than a factor of 2 for the maximum value divided by 95%-percentile value of the Vrmsmax-value. This indicates that a small percentage of freight wagons gives extremely high Vrmsmax vibration values and if these freight wagons could be maintained the maximum value of a freight train could decrease considerably by around a factor of 2 (6 dB).

The Swedish measurements carried out in the frame of work package 2.3 (deliverable D2.8) are analysed differently (whole train passage). Just little more scattering for freight than for Intercity trains is seen.

A LCC analysis is presented at the end of this document. The calculations of the LCC at the wheelsets are based on the mileage-dependent removal of material due to wear on the wheels. The vehicles considered here are type Re420 locomotives. The dominant damage to the wheel treads are polygon formation and rolling contact fatigue. The aim of the LCC study was to determine the capability of different steel grades for the wheels. The steel quality of the product Excellent, with

greater hardness, reduces the cost of the wheels per kilometre by 25 %. 16 % of the costs incurred for the reprofiling and 84 % for the replacement of the wheelsets.

It turns out that even slightly smaller diameter reduction in the reprofiling, higher wear resistance in service and somewhat more prolonged reprofiling intervals have a significant cost saving. Due to steel grades with greater hardness, the two indicators of wear and rolling contact fatigue can be positively influenced. Since the cost of the reprofiling are significantly lower than those for the wheel replacement it should be examined whether the total cost can be significantly reduced by more frequent reprofiling. So it can be concluded that maintaining the wheels at a better OOR level does not necessarily lead to an increased LCC.

2. TABLE OF CONTENTS

1. Executive summary	3
2. Table of contents	5
3. Introduction.....	7
4. Test train in Dottikon and Brunnen	9
4.1 Measurement results Dottikon	9
4.2 Measurement in Brunnen.....	13
4.2.1 Site characterization.....	13
4.2.2 Processing vibration measurements	13
4.2.3 Vibration measurements	17
4.2.4 Dynamic wheel load measurements	18
4.3 Conclusion.....	19
5. Long term Measurements in Brunnen.....	20
5.1 Out of roundness measurements.....	20
5.2 Analysis of vibration measurements Brunnen.....	22
5.2.1 Vibration spread locos.....	22
5.2.2 Vibration spread freight wagons.....	23
5.2.3 Vibration spread passenger wagons.....	23
5.2.4 Time history of some remarkable locomotives	25
5.3 Conclusions	27
6. Other Vibration measurements	28
6.1 Vibration measurements in Sweden	28
6.2 Further RIVAS measurements in Switzerland.....	30
6.2.1 Measurements in Thun.....	30
6.2.2 Measurements in Ligerz.....	32
6.2.3 Measurements in Cadenazzo.....	33
6.2.4 Comparison of the three sites	34
6.3 Conclusions	36
7. Life cycle cost analysis	37
7.1 Scope and methodology for the assessment.....	37
7.2 Understanding tread defects of SBB locomotive Re 420	37
7.2.1 Determinant faults causing reprofiling on locomotives Re420.....	37
7.2.2 Contact patch wheel/rail.....	40

7.2.3	Crack propagation.....	41
7.2.4	Damage mechanisms on locomotive Re 420.....	44
7.3	LCC calculation for SBB locomotive Re 420.....	45
7.3.1	Input parameters.....	45
7.3.2	Costs for reprofiling.....	46
7.3.3	Costs for wheel replacements.....	47
7.3.4	Durability diagrams and costs.....	48
7.4	Conclusions.....	51
8.	Final Conclusions.....	52
9.	Literature.....	53
	Annex A Maintenance process.....	54
	Annex B Wheel tread damage guide.....	56

3. INTRODUCTION

The aim of the RIVAS project is to develop cost effective mitigation measures against ground-borne vibration. Because of the high influence of OOR (out-of-roundness) on the emitted vibration (see e.g. RIVAS deliverables D2.2 [1], D5.4 [2] and D5.6 [3]), trains with wheelsets having high OOR amplitudes can be a problem in the vicinity of populated areas. Until now, only few studies address the wheel maintenance as a mitigation measure to reduce vibration.

During the first part of the project, the influence of out-of-roundness on vibration excitation was studied through measurements and numerical simulations (D2.2 [1]). Then, an overview of rolling stock maintenance practices was given in RIVAS D2.7 [4].

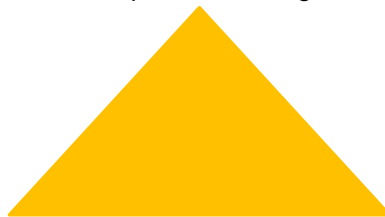
The final step in the project consisted of field tests for evaluating optimised rolling stock maintenance measures. They are described in this document. Three measurement approaches were used:

- (i) A short term test (for both RIVAS WP2 and WP5): Vibration measurements of SBB test train were performed for different velocities at Dottikon (see also further results in D5.6 [3]) and Brunnen. Results are presented in Chapter 4.
- (ii) A long term test: Long term vibration measurements were performed in Brunnen, a major north-south connection between Germany and Italy, for freight and passenger trains at a wheel load checkpoint for nearly six month. Results are presented in Chapter 5.
- (iii) Analysis of existing measurement data: Other measurements performed within RIVAS in Switzerland and Sweden were analysed for evaluating wheel maintenance influence and presented in Chapter 6.

Deliverable D2.7 [4] showed that it is very difficult to give general information for LCC analysis. Different possibilities to improve the out-of-roundness of the trains have to be compared (see also Figure 3.1). Therefore Chapter 7 shows a simple application for a vehicle with higher vibration excitation.

B) Reprofilng in Workshop

- Enough wheel lathe capacity?
- All defects taken away?
- Maintenance plan according to train type?



C) Train type construction

- Passenger wagon
- Problematic passenger/freight wagon
- Problematic Locomotives
- Freight wagon

A) Detection of OOR

- Limit values?
- Which measurements?

Figure 3.1: Maintenance solutions should be chosen depending on the problem.

The strategy for improving wheel maintenance as a mitigation measure is presented in the Figure 3.2 below. The overview study on maintenance of wheelsets can be found in Deliverable D2.7 [4].

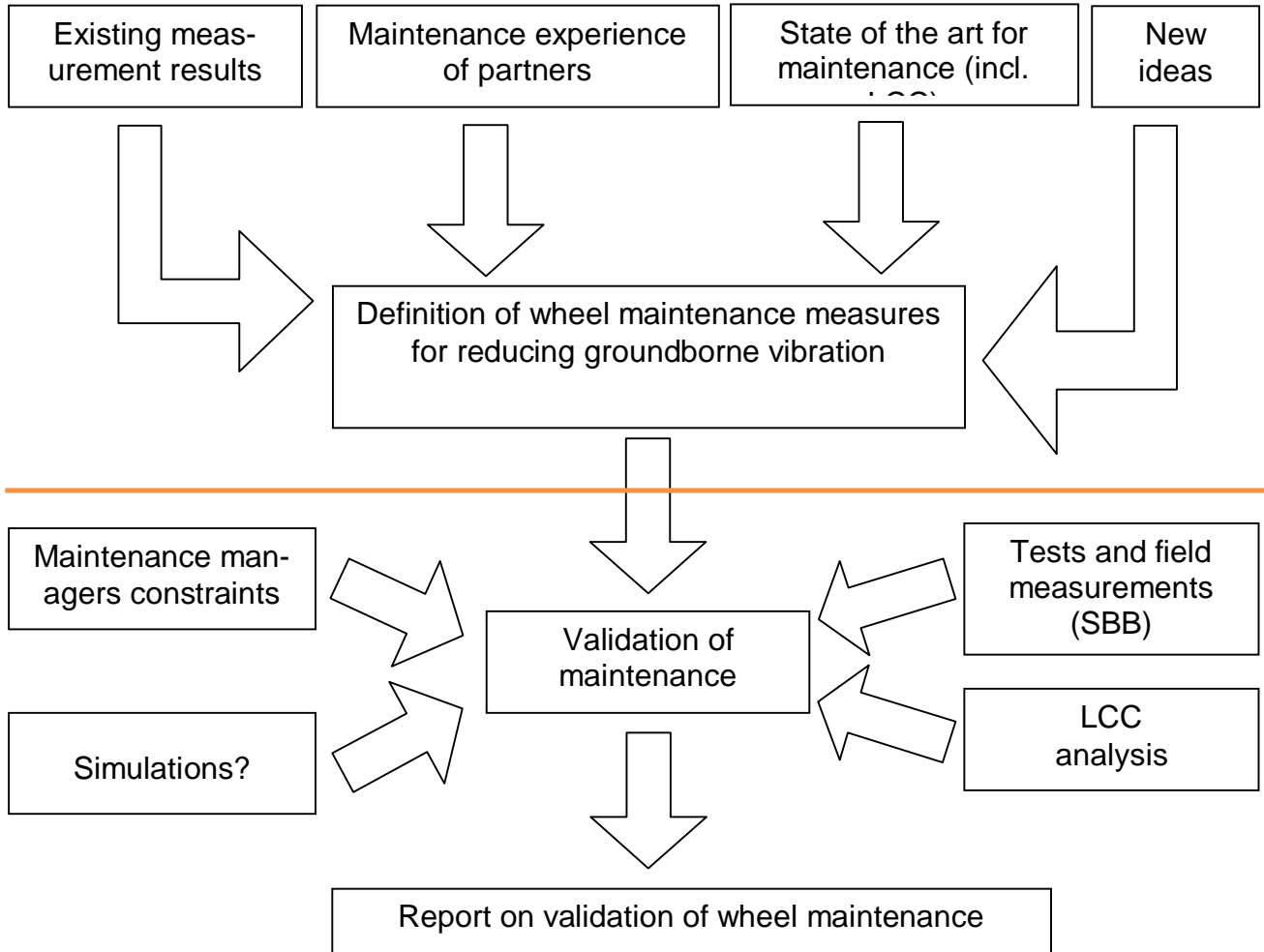


Figure 3.2: Strategy for WP2.4 wheel maintenance project. The first part is covered in RIVAS-Deliverable 2.7, the second part is covered in RIVAS-Deliverable 2.9.

4. TEST TRAIN IN DOTTIKON AND BRUNNEN

A test train, composed to have a sufficient spread in wheel-out-of-roundness among the different wagons so that this influence could be seen in the vibration pass-by measurements, was recorded at different velocities. The tests took place on two sites in Switzerland: In Dottikon (see Section 4.1) by VIBRATEC and in Brunnen (see Section 4.2) by the measurement station used for long term vibration measurements.

4.1 MEASUREMENT RESULTS DOTTIKON

The test train results at Dottikon are shown in Deliverable D5.6 [3]. The test train composition is shown in Figure 4.1 and further details of the test train can be found in [3].

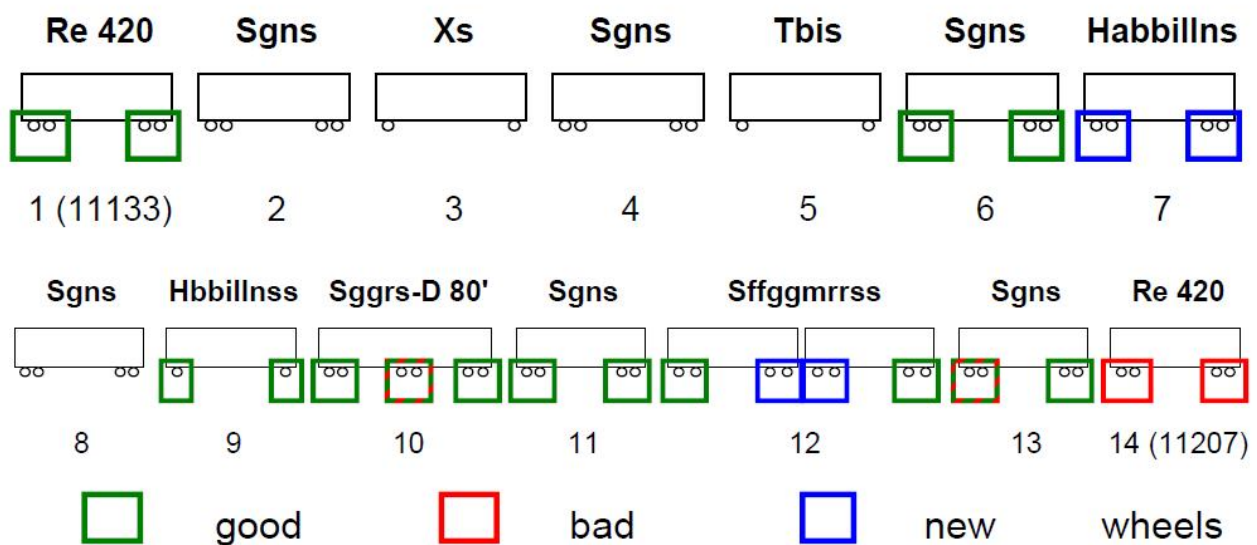


Figure 4.1: Composition of test train, operating in Dottikon [3]

The wheel OOR measurements show that up to a wavelength of about 50 cm both locomotives are dominating the spectrum compared to the freight wagon wheels. At 70 km/h this corresponds to an excitation frequency of 39 Hz and higher. Furthermore the out-of-roundness measurements show high levels of wheel defects on a locomotive already a few weeks after wheel re-profiling.

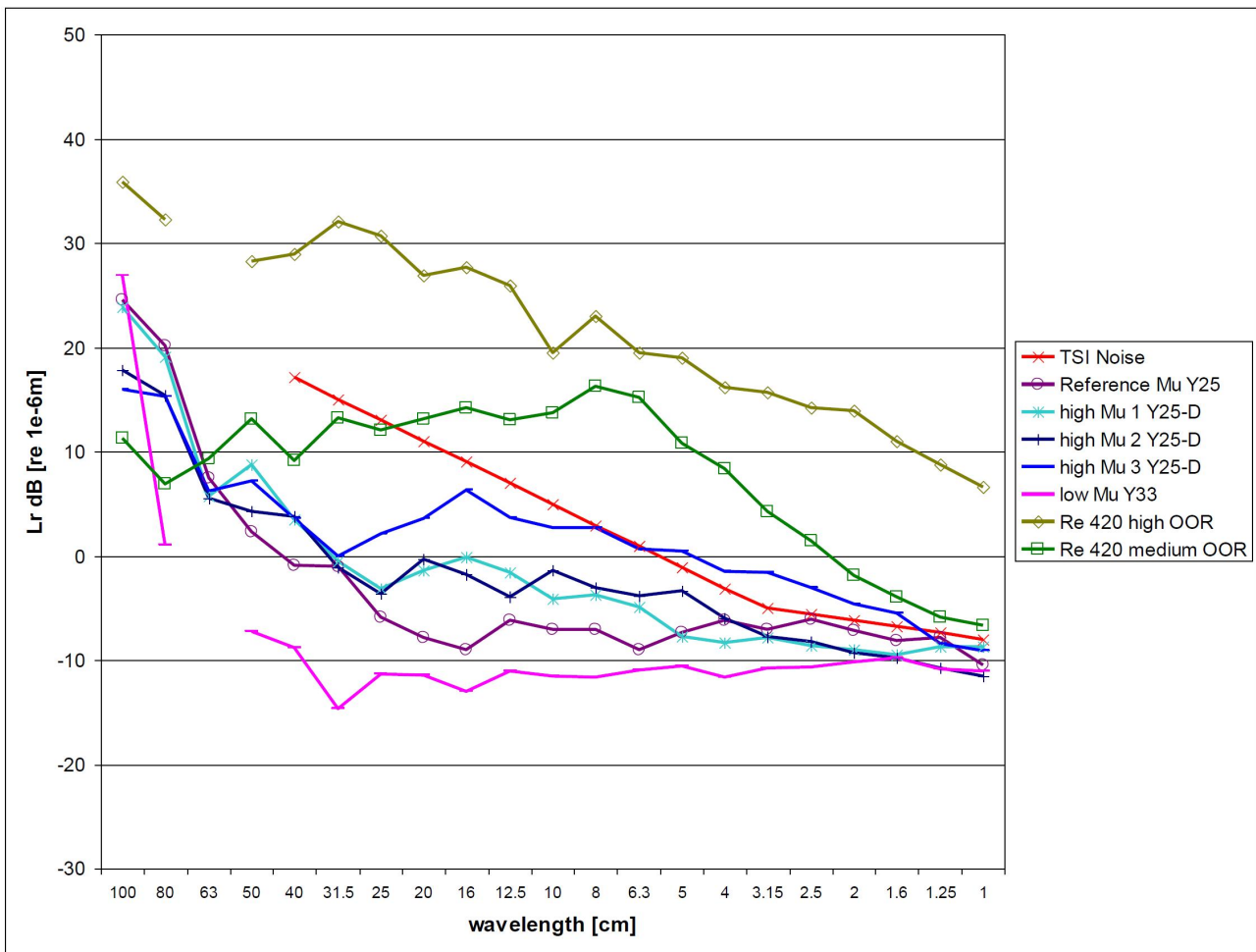


Figure 4.2: Wavelength spectra of different bogies: Y25, Y25-D, Y33 and Loco Re 420 [3].

The wheel out-of-roundness influence on ground-borne vibration is analysed by comparing the vibration spectra of bogies within one freight wagon which have the same design parameters, but different levels of out-of-roundness. However, it can be noted in Figure 4.2 that the levels are just different by around 5 dB.

A comparison of the ground vibration spectrum at 4 m from the track excited by the two different bogies is given in Figure 4.3. The reduced vibration level associated with the removal of out-of-roundness is also presented as the insertion loss. In some frequency bands the difference is zero however by looking at how the difference in vibration level is shifted towards higher frequencies for higher speeds (as is the case with the irregularities in the frequency domain) it is likely that this difference is mainly caused by the differences in wheel tread condition.

A clearer difference due to the wheel OOR maintenance status can be seen in Figure 4.4, where the vibration spectra of the two locomotives, which are of the same type but have significant difference in the wheel condition, are compared. The vibration measurements in the current campaign show that differences of up to 20 dB in some frequency bands is found between good and bad wheels of locomotives which also differ in the OOR measurement for some wavelength up to 20 dB.

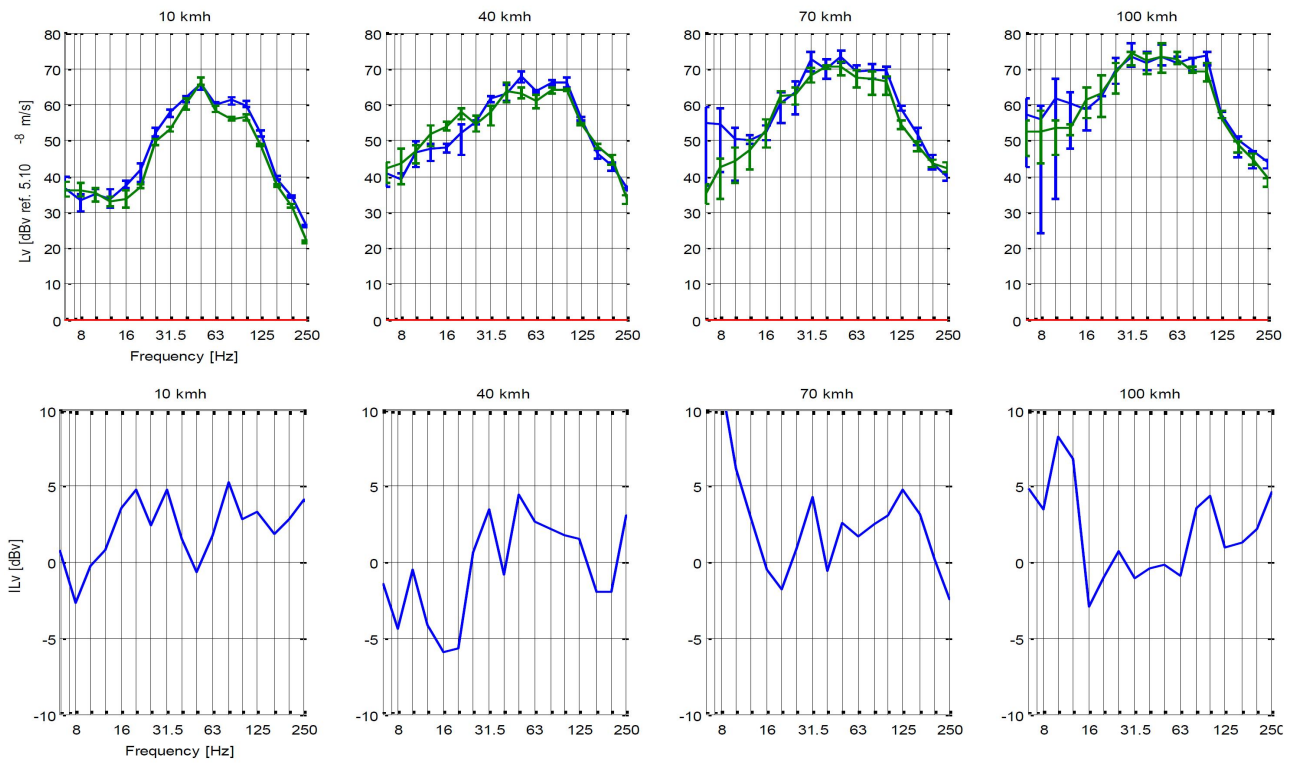


Figure 4.3: Influence and insertion loss from out of round wheels Y25-D boogie 1 and boogie 3 at 4 m distance. [3]

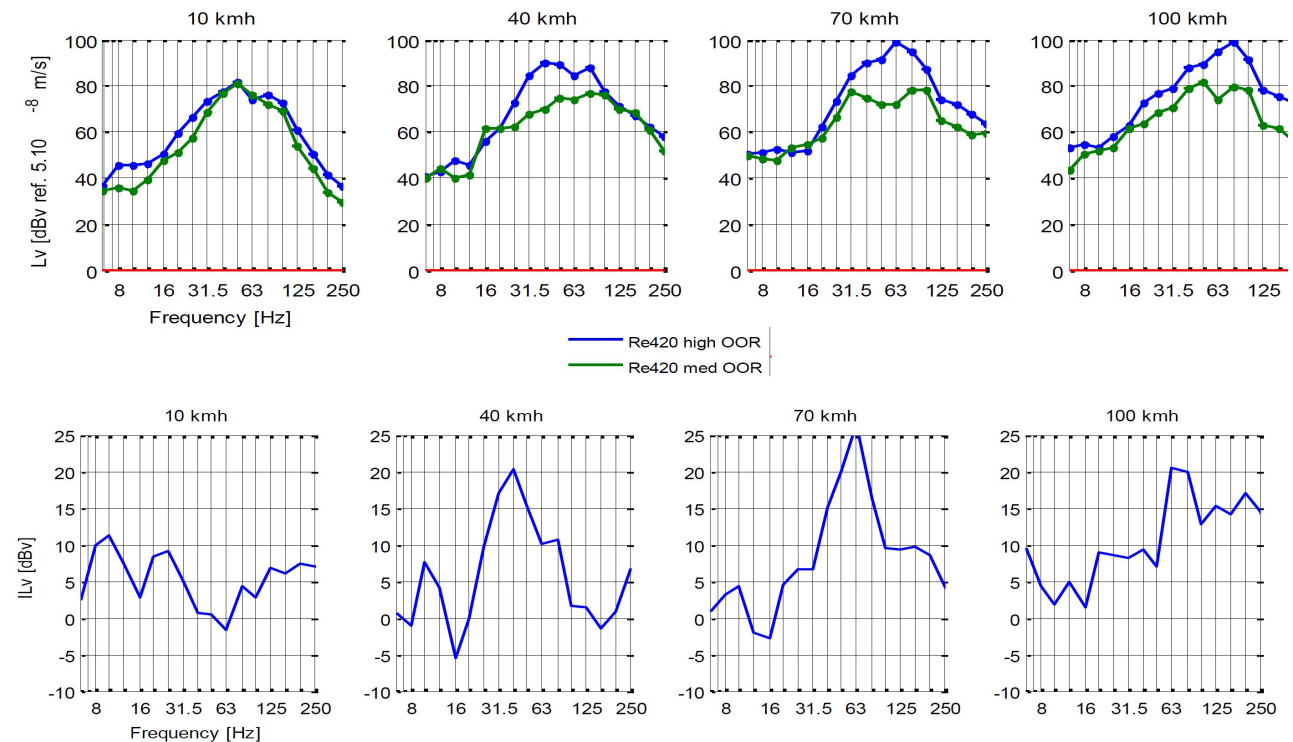


Figure 4.4: Influence of out-of-round wheels on the vibration level generated by the locomotives Re420 at 4 m distance. [3]

The phenomenon of a wheel flat is studied, by comparing the vibration spectra of two bogies of the same type and having similar OOR level, except for one having a wheel flat. Results are shown in Figure 4.5. The ground vibration spectra measured for bogie 2 (with wheel flat) and bogie 1 are presented. The measured insertion loss (IL_v) related to the suppression of the wheel flat reveals that for all considered train speeds and above about 30Hz, the IL is around 5 dB and goes up to 10 dB.

As shown above, the measured out-of-roundness for all wheels of the two bogies are similar, so that only the influence of wheel flat is seen in the insertion loss. One general remark is that the influence of the wheel flat is primarily seen at higher frequencies which is expected considering the impact load generated by the flat on the rail. Furthermore this excitation is shifted towards higher frequencies for higher vehicle speeds which also is expected from an impact load with shorter duration.

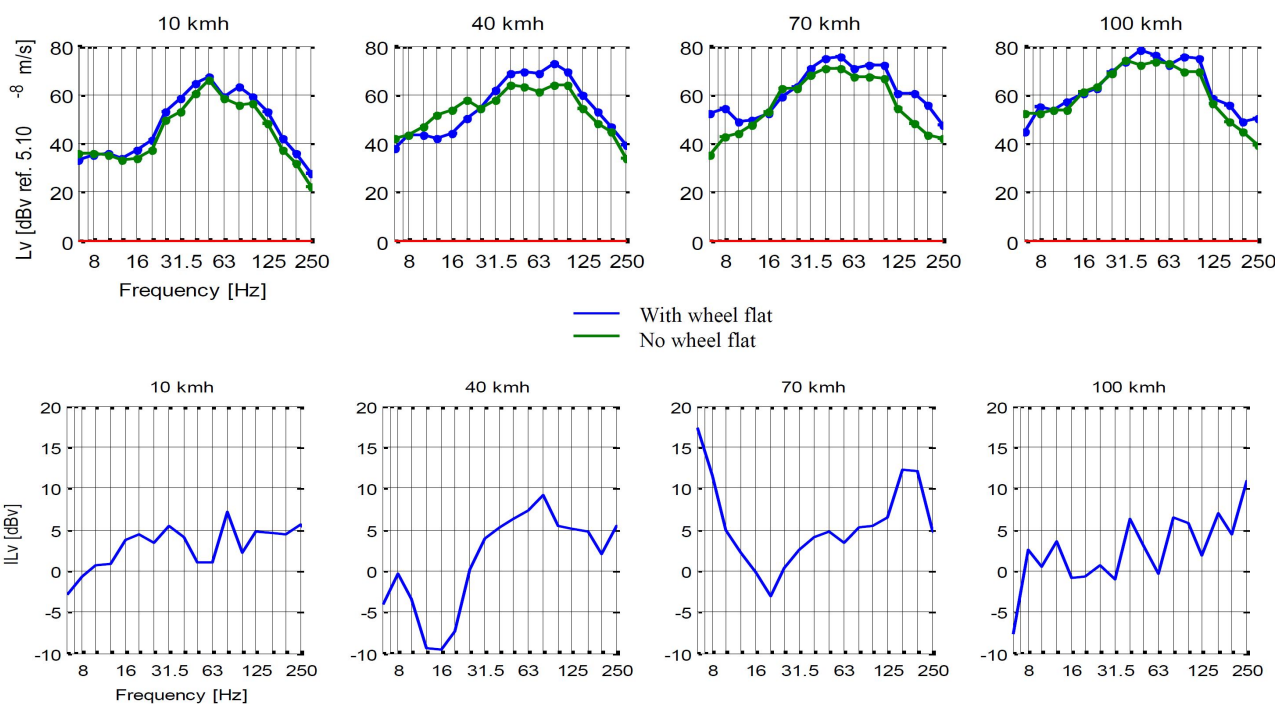


Figure 4.5: Influence of a wheelflat at Y25-D bogie 2 in comparison to bogie 1. [3]

4.2 MEASUREMENT IN BRUNNEN

4.2.1 Site characterization

At the wheel load check (WLC) point of eastern track at km 19.432 4 acceleration sensors were installed, two in 2 m in the ballast (a21, a22) and two in 8 m distance (a81 und a82) under the ground surface next to the track, see Figure 4.6. Sensors a21 and a81 are exactly at the same track km as the first strain gauge and sensors a22 und a82 at the same track km as the second strain gauge of the WLC. The wheel load checkpoint consists of 16 sensors per track.

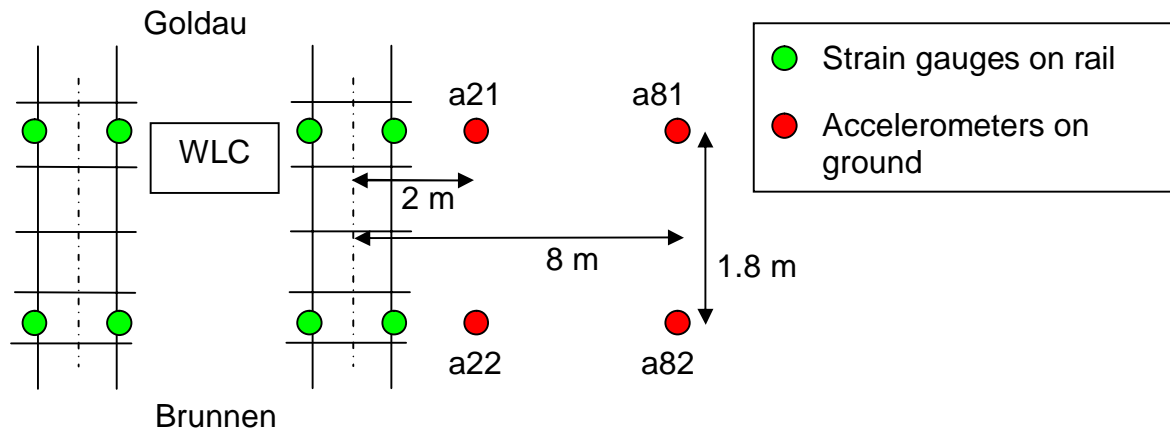


Figure 4.6: Situation map of vibration acceleration sensors, and 8 (of 32) strain gauges on rail.

One sensor in the ballast at 2 m distance (50 g measurement range) and the sensors in 8 m distance (10 g measurement range) are shown in Figure 4.7. The anti-aliasing filter at the amplifier was 500 Hz and the signal sampling rate was 10 kHz.



Figure 4.7: Photos of acceleration sensors at 2 m, left photo, and 8 m, right photo.

4.2.2 Processing vibration measurements

For each train pass-by, two types of information are stored, the raw data files with train information and a summary of vibration results (vrmsmax, vLEQ, 1/3-octave FFT) in a excel sheet.

Each line of the excel sheet contains the data for an individual axle; the axle load and the wheel forces are determined and passed to the excel sheet. Additional available information is as follows:

- time of pass-by
- train number
- train type (freight, passenger)
- total number of axles in train
- wagon number (if available)
- wagon type
- total number of axles in wagon
- current axle number
- velocity
- location of the raw data file

For each complete train pass-by, one set of raw data files is generated. These contain among others:

- the position of each axle in the signals (expressed in samples), for each of the sensors on the track
- the acceleration signals measured by sensors a21, a22, a81 and a82.

Based on the information from the excel file and the raw data, it is possible to calculate for each pass-by the vibration levels of the four measurement points. Since for most pass-bys, wagon numbers are available, vibration levels are calculated for each wagon, instead of for the whole train. This allows a comparison of vibration level for a specific wagon number.

The procedure for processing the data in Matlab® (Mathworks, Boston, USA) is as follows:

- Each line of the excel sheet is read. For each wagon, the first and last axle are determined.
- The first and last sample in the vibration signal, corresponding to the current analysed wagon, is determined based on the axle positions.
- An additional number of samples is added to the first and last axles for analysis, corresponding to a displacement of the train of 2 m. The corresponding number of samples can be determined since the velocity of the train is given in the excel sheet. The resulting selection is shown in Figure 4.8, showing the signal of an accelerometer at 2 m, with the vertical lines indicating the first and last sample for analysis of each wagon, each colour representing a different wagon. From that Figure 4.8, it is clear that due to the addition of samples corresponding to a train displacement of 2 m, the signals for different wagons overlap.

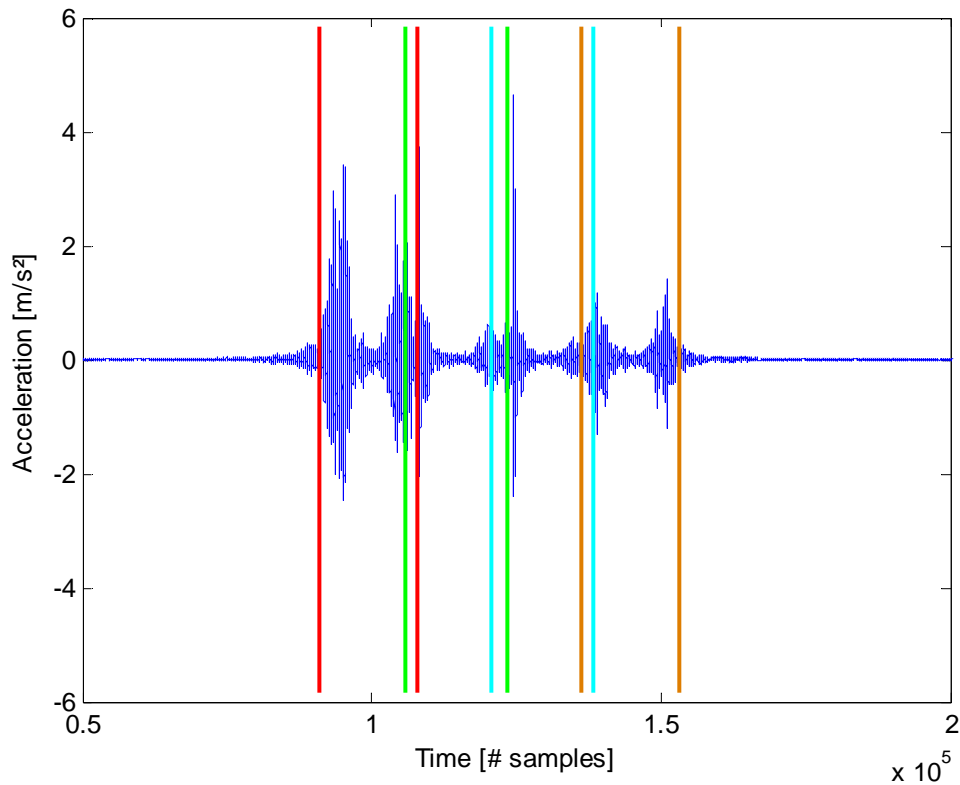


Figure 4.8: Signal selection for each wagon

- After selection of the signals for a given wagon, the signal is integrated to velocity, the overall average vibration level between 4 and 250 Hz is calculated (average RMS level), as well as the maximum RMS level. The average third octave band levels between 4 and 250 Hz are calculated as well.
- The vibration data values, expressed in dB respective 1E-9 m/s are added to the excel sheet.

Figure 4.9 shows an example of the resulting excel sheet. The data on the left (indicated in red) is the original data. The data on the right (indicated in green) is the vibration data added after processing, the blue rectangles indicating the data for the individual accelerometers (four in total). Data is added to the first row of a wagon, the rows corresponding to the remaining axes of that wagon are left blank.

4.2.3 Vibration measurements

The test train was also running in Brunnen at the wheel load checkpoint (WLC) and measured by the long term vibration measurement station. Some results of these test train measurements are shown here to verify the influence of out-of-roundness.

In Figure 4.10 the mean emission spectra for the two locomotives of the test train at 2 m and 8 m distance is shown. A clear velocity dependency is visible between 10, 40 and 70 km/h, unfortunately for security reasons 100 km/h was not possible to run. Instead 80 km/h was run but does not show significant differences in amplitudes.

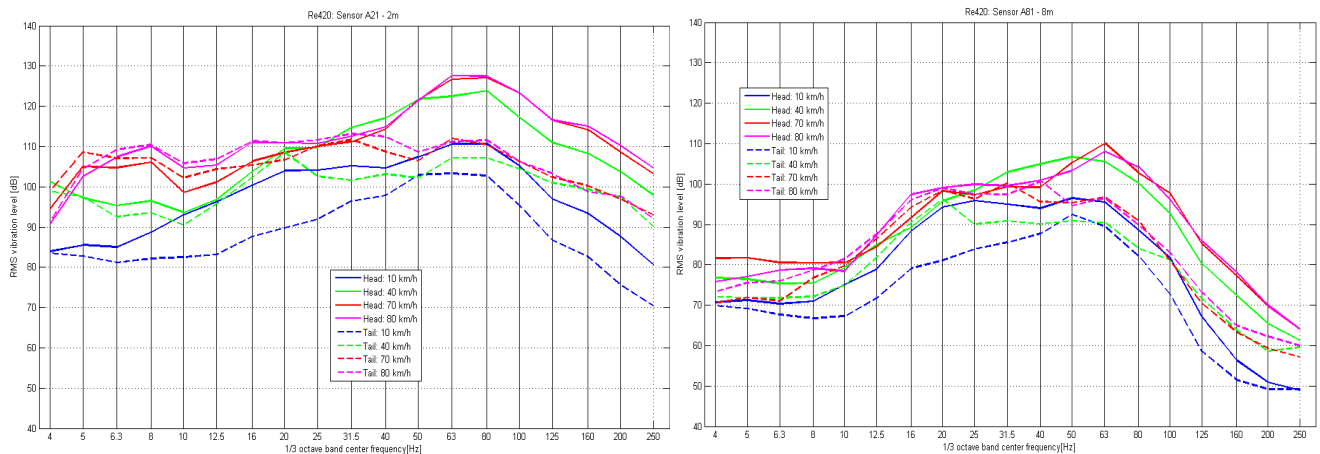


Figure 4.10: Emission spectra from the locomotives Re420 in 2 m (left) and 8 m distance (right).

A clear difference in vibration level due to maintenance status of wheel out-of-roundness can be seen by comparing the vibration spectra of the two locomotives, see Figure 4.11. This Figure 4.11 can be compared to Figure 4.4 and it can be seen that the absolute value of insertion loss is about the same in both cases, between 15 and 20 dB. The frequency behaviour is not fully the same. A reason could be that the train-track interaction is different between Dottikon and Brunnen.

In Figure 4.12 the emission spectra of regular locomotives Re420 are compared with the test train locomotives for 80 km/h. The locomotive “Head” with high OOR on the one hand is similar to the 95% value of regular pass-byes. The locomotive “Tail” on the other hand is normally better than the median value above 40 Hz. This is due to the recent maintenance only few weeks before the measurement took place.

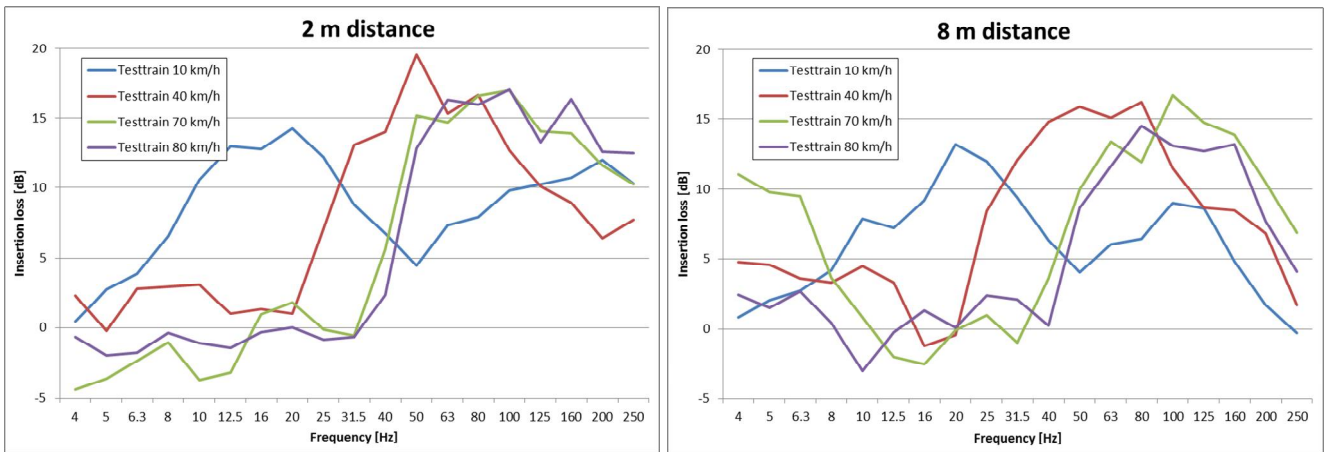


Figure 4.11: Insertion loss spectra from the locomotives Re420 at 2 m and 8 m distance.

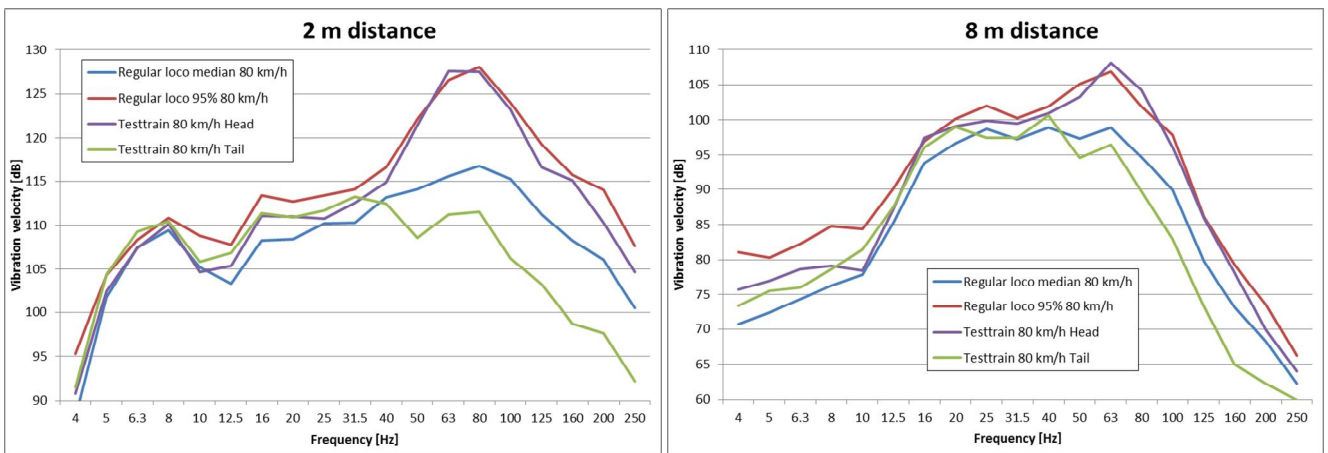


Figure 4.12: Emission spectra from regular locomotives Re420 as well as test train locos (Head, Tail) at 2 m and 8 m distance.

4.2.4 Dynamic wheel load measurements

A comparison of vibration measurements with WLC (wheel load checkpoint) measurements is possible as both measurement equipment were running during the test train measurements. Figure 4.13 shows the test train results in Brunnen and Figure 4.14 shows the test train results in Dottikon for every wheel. For the WLC measurements the arithmetic mean of the maximum dynamic force was taken for the 70 km/h test runs, and the static load was then subtracted. A clear difference in amplitudes is observed for the two locomotives of around a factor 4 which would correspond to 12 dB, around the effect of maintenance observed in section 4.1 and 4.2.

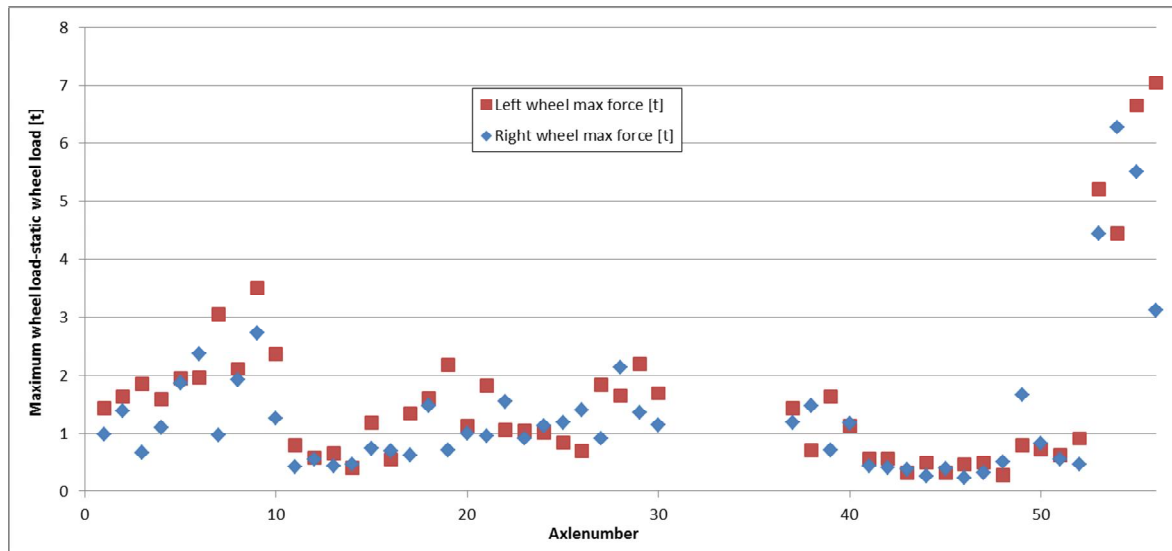


Figure 4.13: Brunnen mean maximum wheel load minus static wheel load for 70 km/h. (The wagon with axle 21-26 was not running in Brunnen, but can be seen in Dottikon)

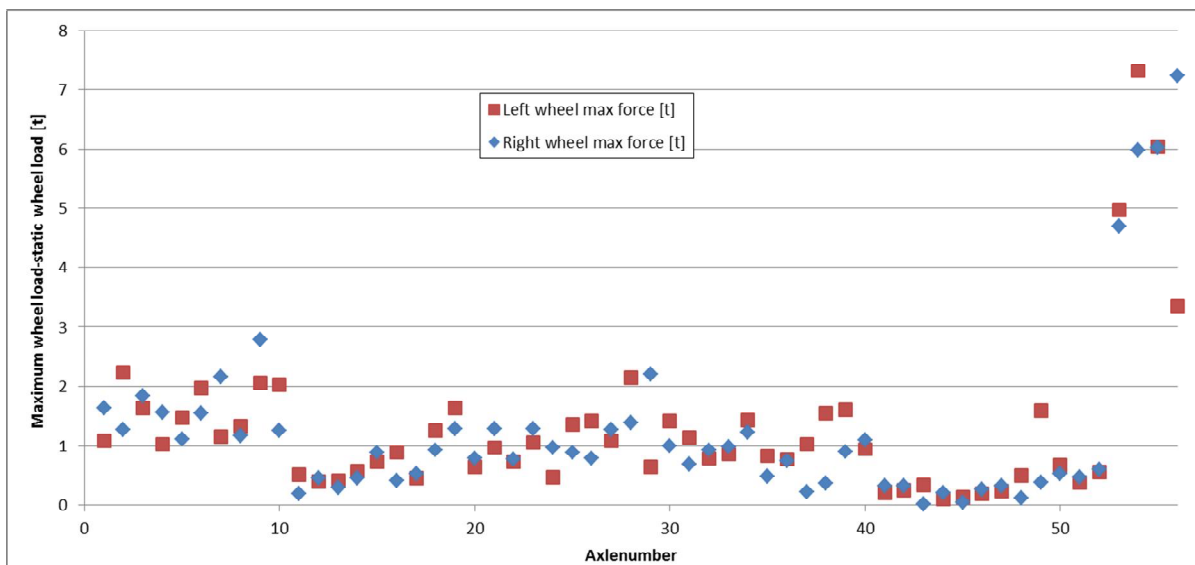


Figure 4.14: Dottikon mean maximum wheel load minus static wheel load for 70 km/h.

4.3 CONCLUSION

The wheel out-of-roundness has a significant influence on the vibration emissions. Furthermore the out-of-roundness measurements show high levels of wheel defects on a locomotive only a few weeks after wheel reprofiling.

A reduction of the combined wheel and rail irregularities with an amount of X dB by removing wheel out-of-roundness will roughly reduce the ground vibration with around an amount of X dB. The measurements of wheel out-of-roundness in the current campaign show that differences of up to 20 dB is found between good and bad wheels of the locomotives used in this campaign (type Re420). Dynamic force measurements show similar amplitude reductions for the two test train locomotives.

5. LONG TERM MEASUREMENTS IN BRUNNEN

The long term measurement results are shown in this Chapter.

5.1 OUT OF ROUNDNESS MEASUREMENTS

In Deliverable D2.4 [5] the out-of-roundness of locomotives Re420 and Re620 are analysed. The measurements of OOR (out of roundness) are not taken at a specific moment, so they show more or less the spread of the fleet circulating in Switzerland. In Figure 5.1 the mean, median and 95% values are shown from over a thousand wheel OOR measurements. It can be seen that both locomotive types differ just little and that the higher differences are found for wavelengths above 40cm.

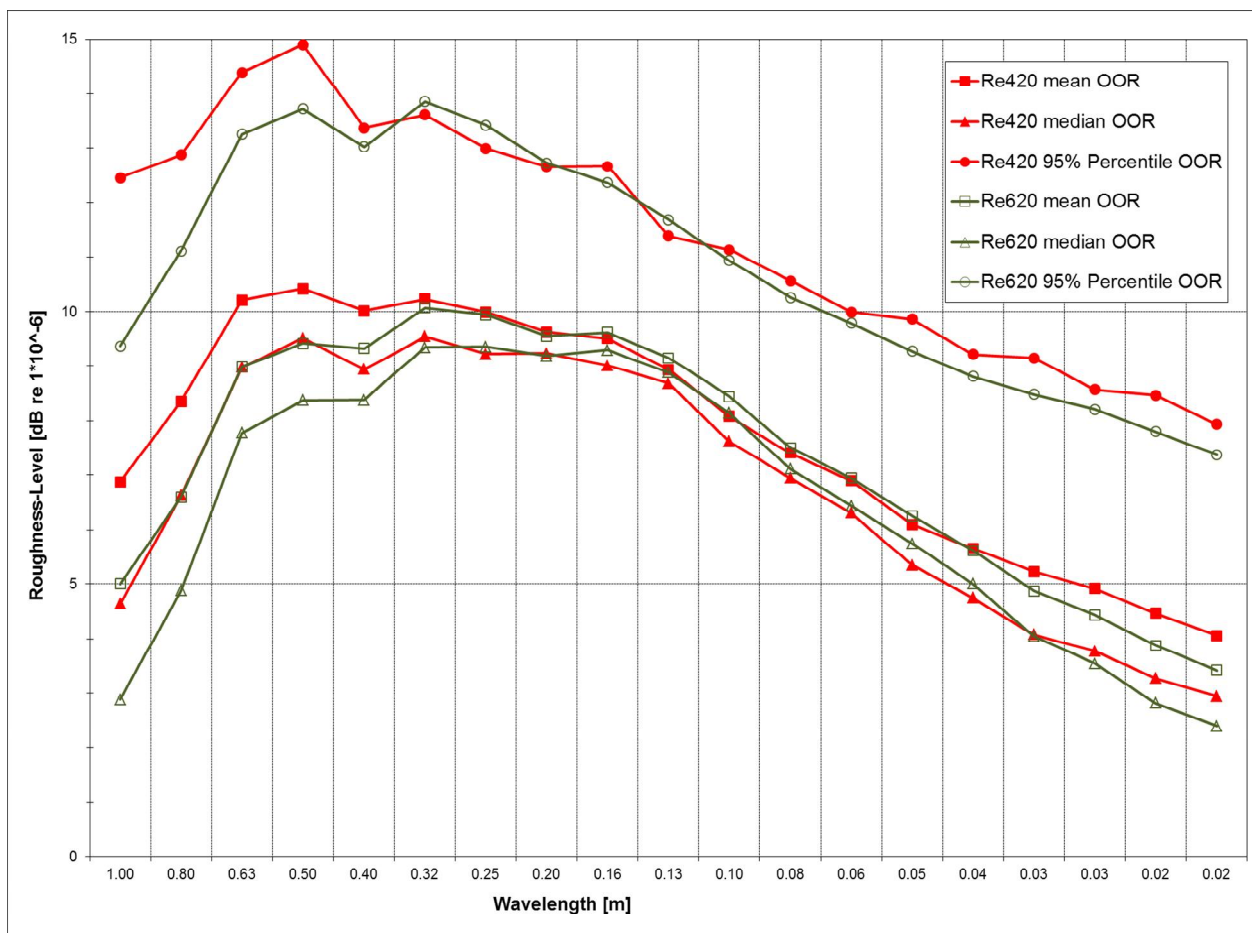


Figure 5.1: Roughness level of mean, median and 95%-percentile of locomotives Re420 and Re620.

Figure 5.2 shows the results of the difference between 95%-percentile and median value. The difference is for both locomotives similar and is around 6 dB at 0.5 m and longer wavelengths.

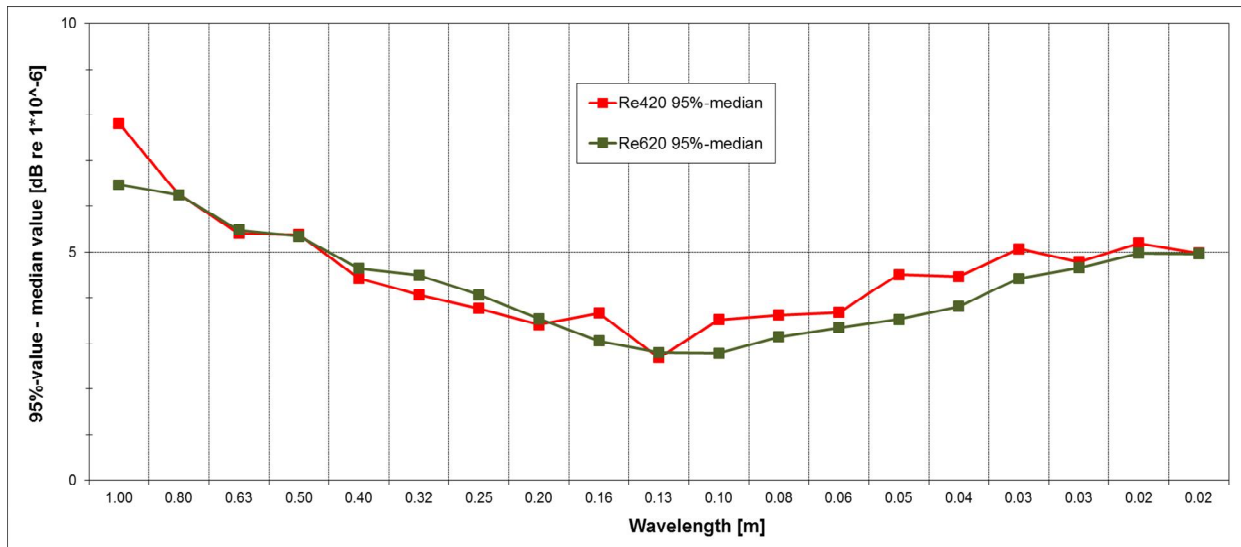


Figure 5.2: Roughness level difference of 95%-percentile and median values of OOR of locomotives Re420 and Re620.

A comparison of the OOR measurements of the Re420 and the vibration measurements of regular Re420 pass-bys in Brunnen is done in Figure 5.3. The OOR measurement of wavelength is transferred into frequency by supposing 110 km/h train velocity. It can be seen that at 40-63 Hz the influence of OOR is quite well represented by the vibration measurements.

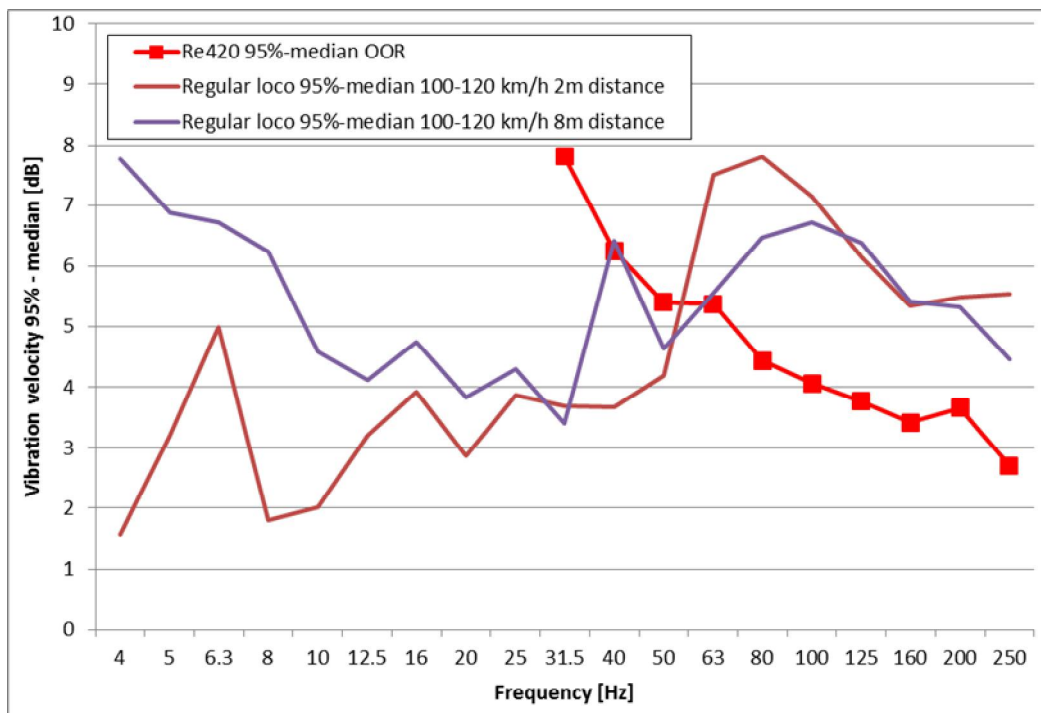


Figure 5.3: Roughness level difference of 95%-percentile and median values of OOR of locomotives Re420 in comparison to measurements in 2 m and 8 m distance in Brunnen.

5.2 ANALYSIS OF VIBRATION MEASUREMENTS BRUNNEN

5.2.1 Vibration spread locos

The spread on third octave band spectra is compared for different train types. Since the train velocity has an effect on the overall level and the pass-by spectrum, the comparison is based on pass-bys with similar velocities, see as an example vibration velocity spectra for Re420 at 2 m and 8 m distance in Figure 5.4. The vibration spectra of all pass-bys in the considered velocity range are shown.

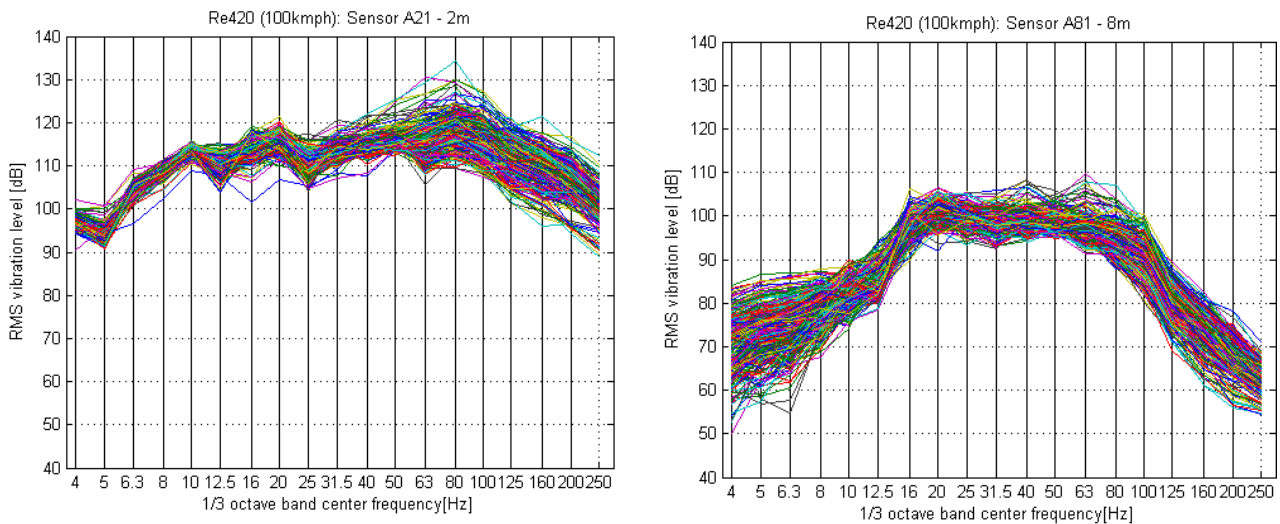


Figure 5.4: Re 420 100 km/h, 2 m and 8 m distance

The median value for each third octave band, as well as the 95 % percentile is shown in Figure 5.5 for the velocity range of 100-120 km/h.

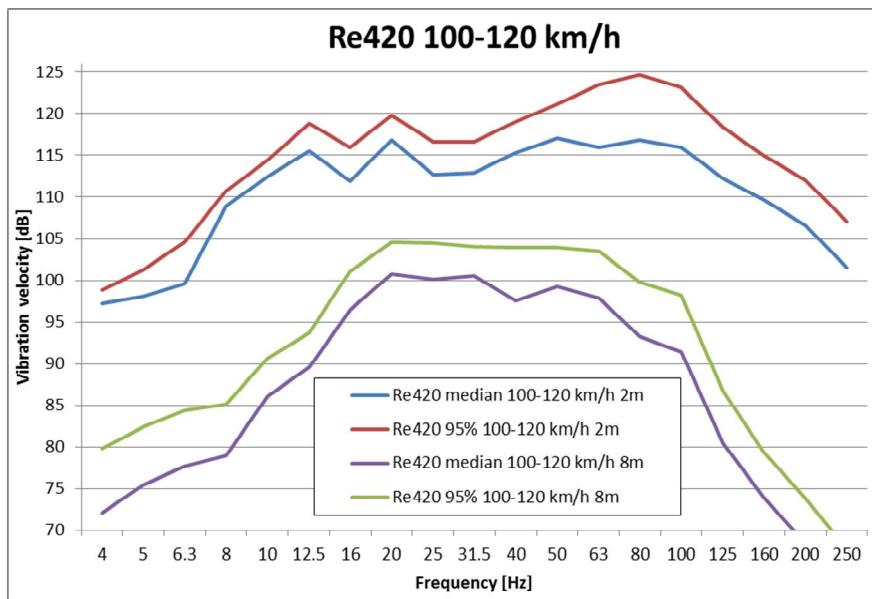


Figure 5.5: Loco Re 420 100-120 km/h, median and 95%-percentile at 2 m and 8 m distance

5.2.2 Vibration spread freight wagons

The freight wagon type Sgns is used quite frequently for freight traffic and is also used for the test train. In Figure 5.6 the result of a first analysis shows the 95%-percentile and the median value for train velocity of 75-85 km/h. Above 63 Hz the difference between 95%-percentile and median shows a growing difference.

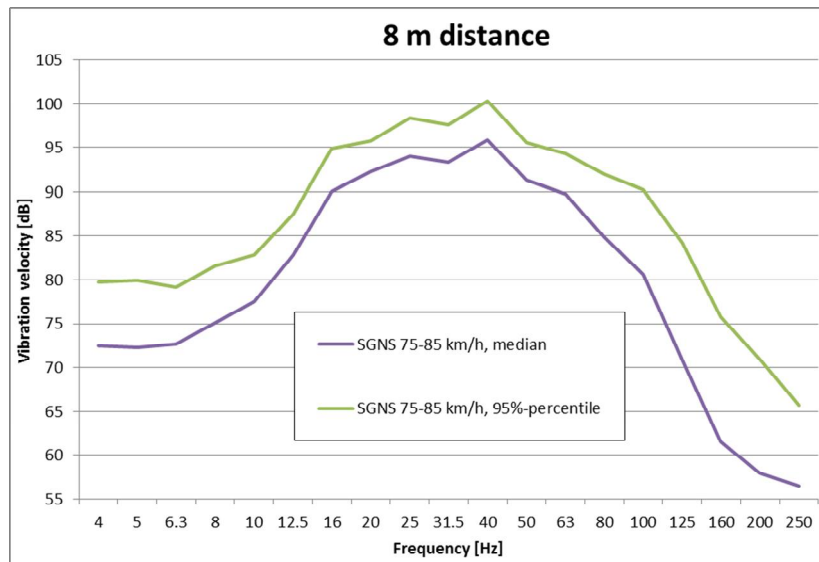


Figure 5.6: Freight wagon Sgns 75-85 km/h, median and 95%-percentile at 8 m distance

5.2.3 Vibration spread passenger wagons

For the analysis of the vibration spread the ICN tilting train are compared with regional trains Domino and regional train Flirt. All are disc braked and for each train type there is one wagon with accelerated wheelset and one wagon with non-accelerated wheelsets.

Figures 5.7 and 5.8 illustrate the median value of the vibration velocity at 2 m and 8 m. At 20 Hz and higher frequencies the Domino with accelerated wheels demonstrate higher vibration values of about 5 dB. On the other hand the Domino without accelerated wheels shows quite low values for lower frequencies. The other two wagon types have, for 2 m and 8 m distance, similar values and do not differ as much as for the Domino.

Figure 5.8 illustrates that the ICN has the lowest values between 31-80 Hz which is probably due to a regular check of wheel OOR-status every two weeks (0.5 mm).

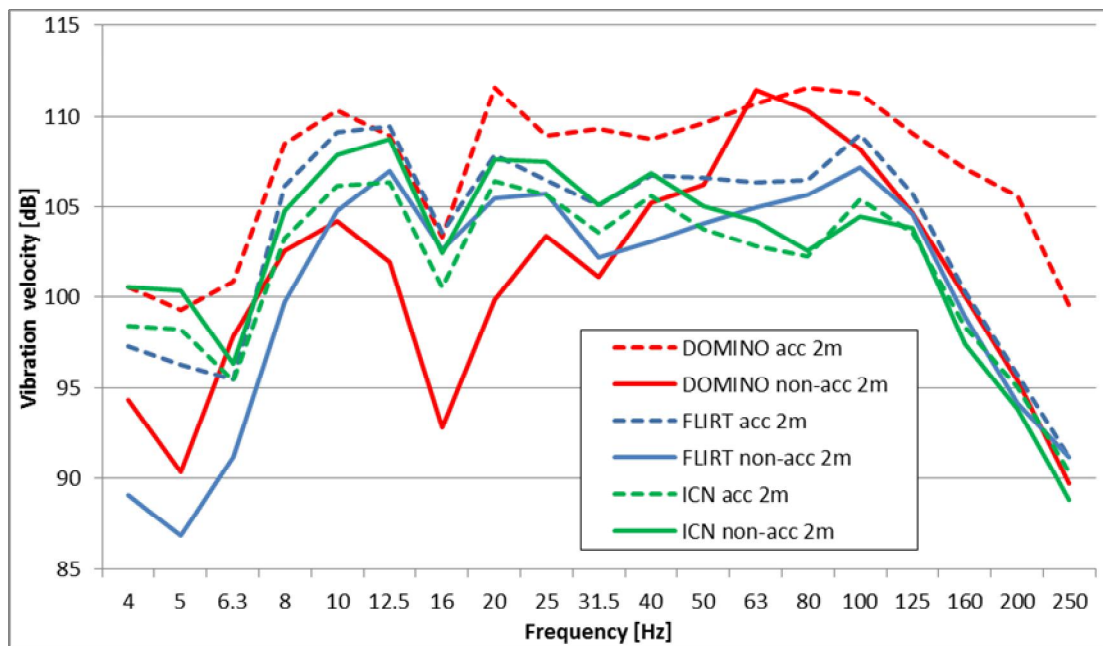


Figure 5.7: Domino, Flirt and ICN for 100-120 km/h median vibration velocity at 2 m distance.

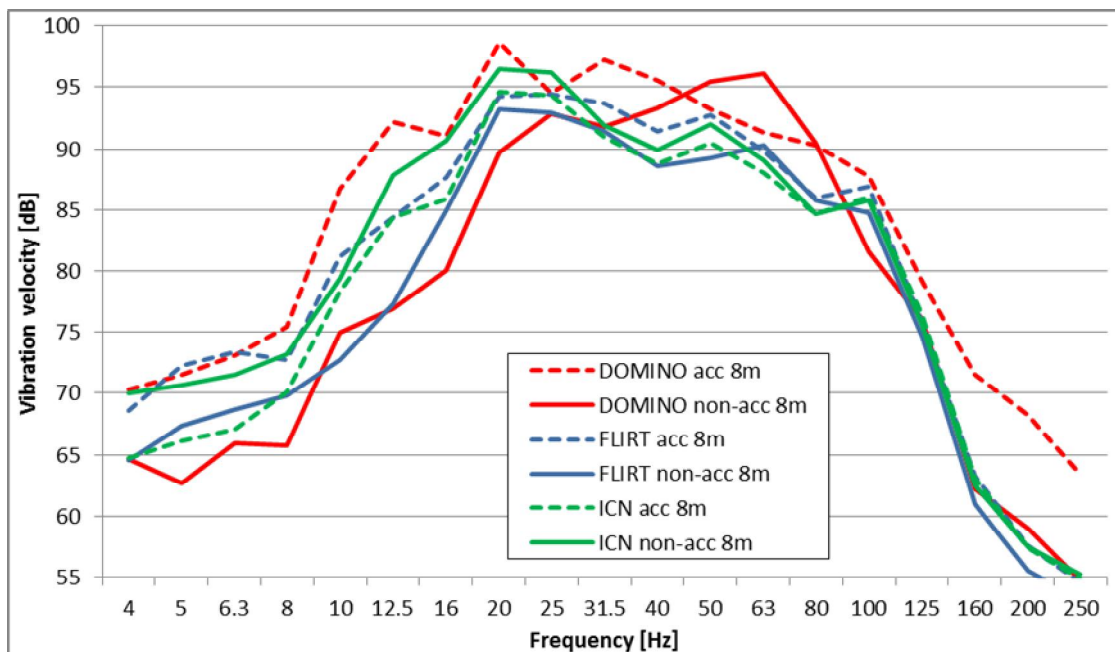


Figure 5.8: Domino, Flirt and ICN for 100-120 km/h median vibration velocity at 8 m distance.

The Figures 5.9 and 5.10 show the differences between the 95-percentile value and the median value at 2 m and 8 m distance. It seems that the non accelerated wheelsets of Flirt and Domino show larger differences at around 63 Hz which is most probably due to out-of-round wheels.

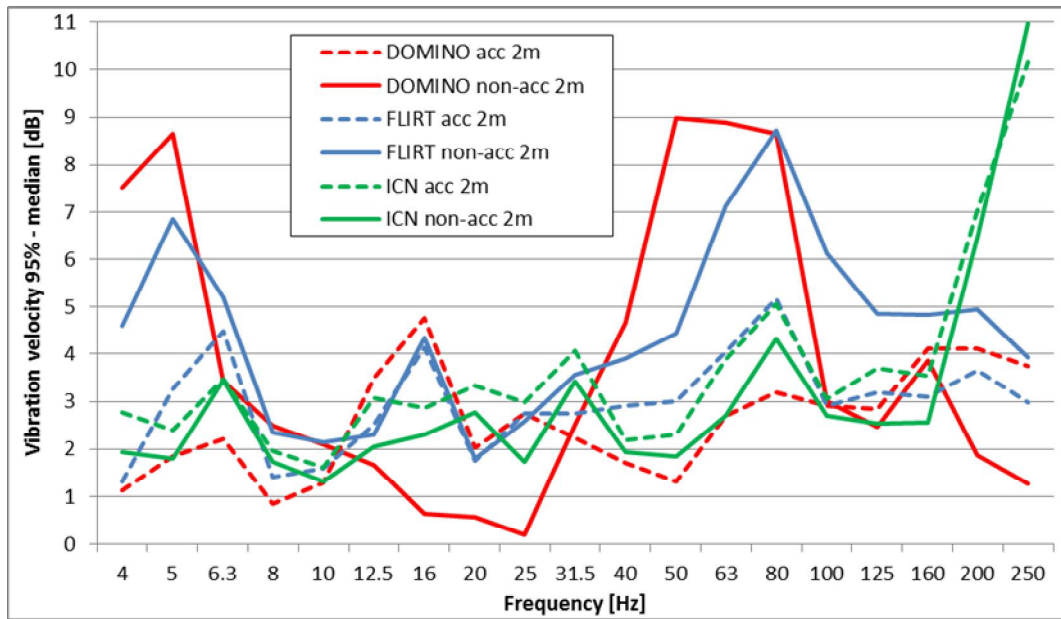


Figure 5.9: Domino, Flirt and ICN for 100-120 km/h, 95%-value minus median vibration velocity at 2 m distance.

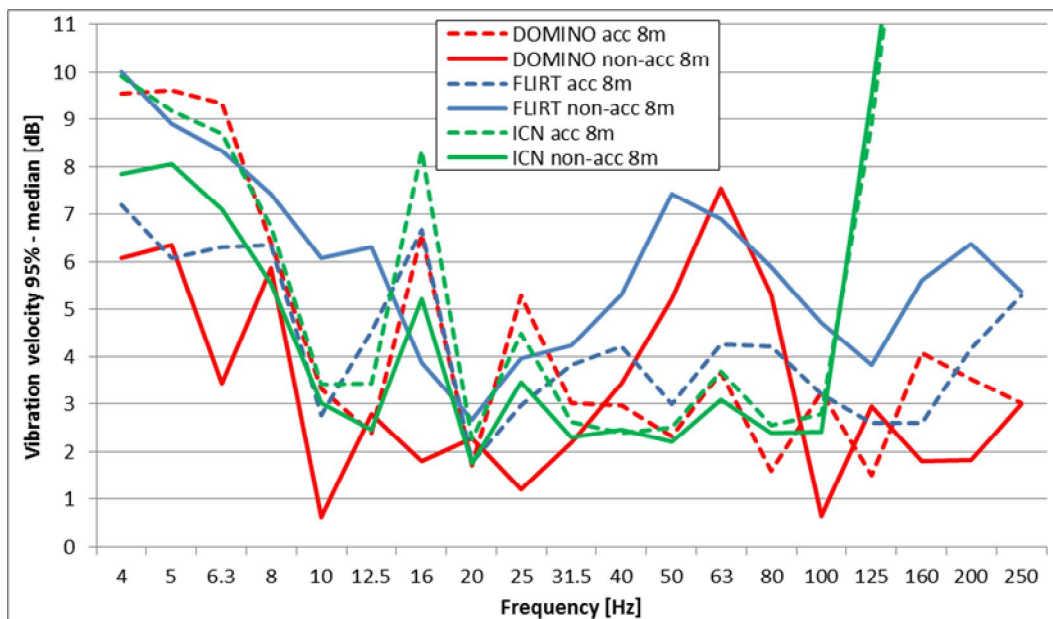


Figure 5.10: Domino, Flirt and ICN for 100-120 km/h, 95%-value minus median vibration velocity at 8 m distance.

5.2.4 Time history of some remarkable locomotives

Figures 5.11 and 5.12 show the time history of the V_{rmsmax} at 2 m and 8 m distance of five locomotives Re420 (90-130 km/h) over the measurement period in Brunnen. In both figures the moment of maintenance shows significant reduction of vibration values.

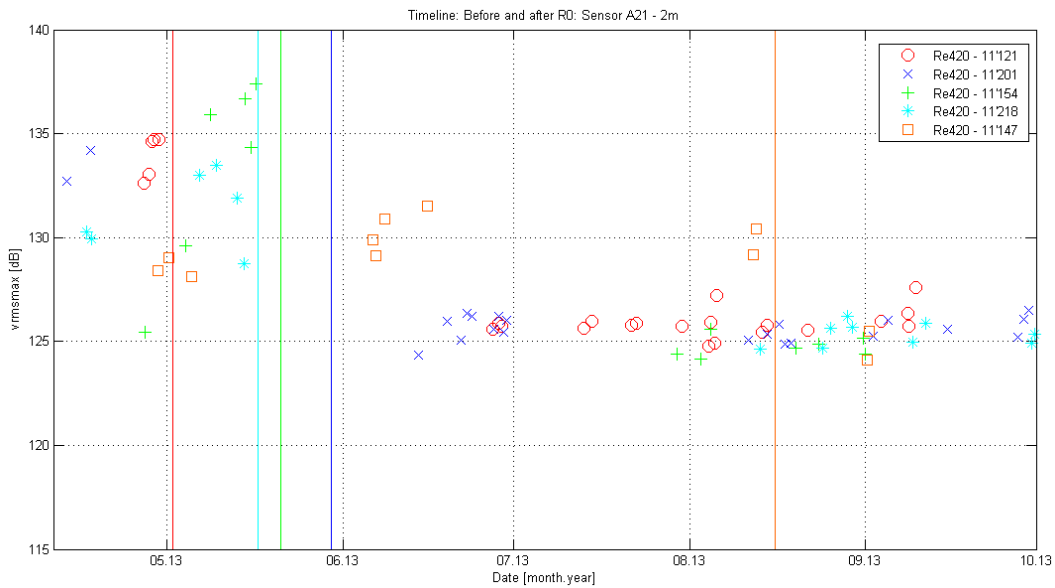


Figure 5.11: V_{rmsmax} time history for 2 m distance of 5 locomotives Re420 (90-130 km/h) and their maintenance date illustrated with vertical coloured line.

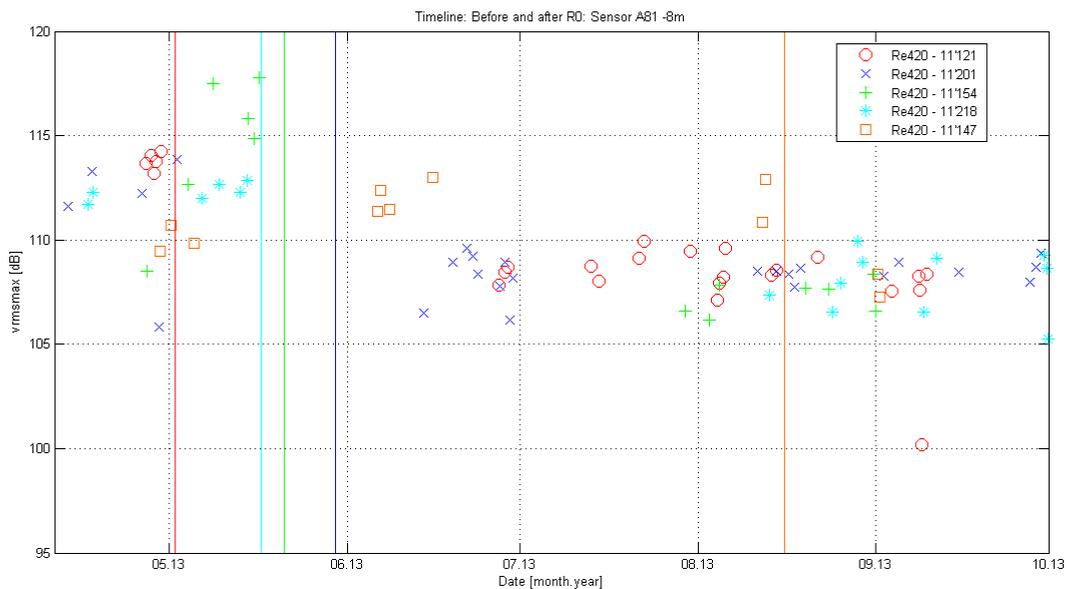


Figure 5.12: V_{rmsmax} time history for 8 m distance of 5 Locomotives Re420 (90-130 km/h) and their maintenance date illustrated with vertical coloured line.

Figure 5.13 and 5.14 show the insertion loss calculation at 2 m and 8 m distance of the 5 locomotives Re420 by comparison of measurements before/after the maintenance date. At 2 m distance a significant reduction of vibration values can be seen above 20 Hz and for 8 m distance above 25 Hz. The insertion loss can reach up to 12 dB.

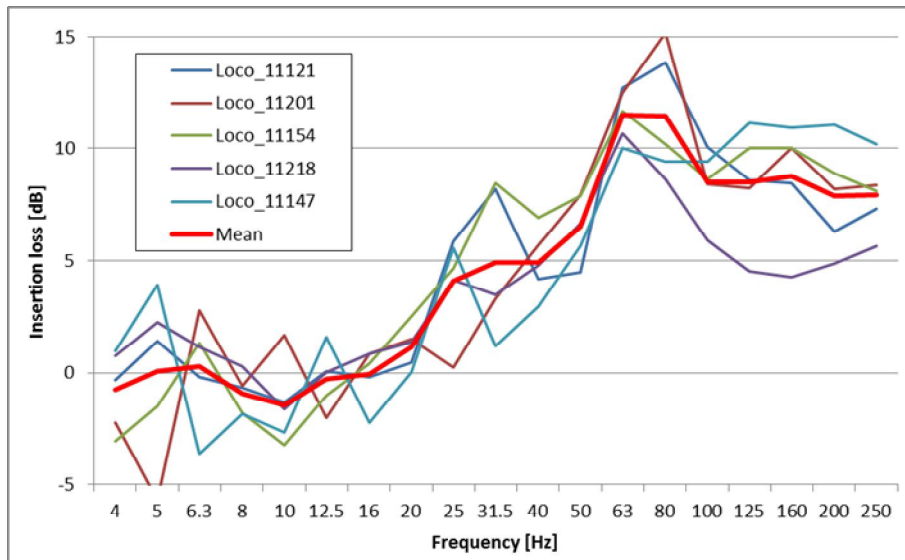


Figure 5.13: Insertion loss at 2 m distance of 5 Locomotives Re420.

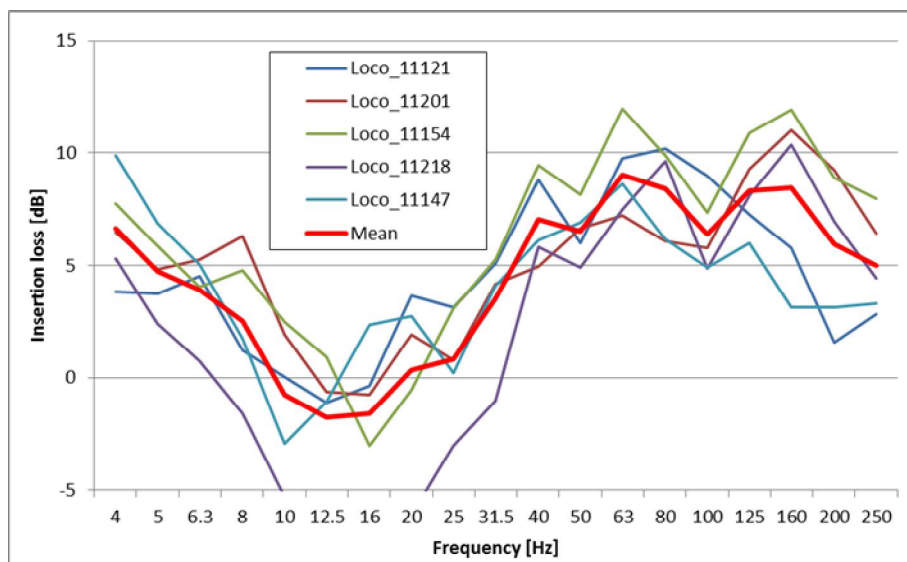


Figure 5.14: Insertion loss at 8 m distance of 5 Locomotives Re420.

5.3 CONCLUSIONS

The comparison of OOR measurements presented in D2.2 [1] and vibration measurements show a good correlation. The scattering (95%-median value) for different vehicle types is shown and demonstrates a potential for improvement by maintenance. The insertion loss for some of the Re420 vehicles could be validated and have reached values up to 12 dB. The Intercity trains which are maintained more regularly to reduce structure borne noise in the vehicle show a lower potential. A comparison of passenger coaches with driven wheelsets and non driven wheelsets show especially for the SBB regional trains (Domino but also for the Flirt) more vibration for driven wheelsets. The vibration spread for CARGO wagons is similar to the Locomotive Re420 and shows potential for maintenance.

6. OTHER VIBRATION MEASUREMENTS

6.1 VIBRATION MEASUREMENTS IN SWEDEN

In Sweden vibration measurements were performed during the RIVAS project for mitigation measures tested for Trafikverket, see e.g. [6]. Some of the measurements are shown here to make a small analysis on vehicle spread of vibration results and to have an indication on the spread of wheel conditions.

Results of measurements before installing the sheet piling wall for 10 passenger train X31 at speed 77 km/h \pm 5%, at 8 m distance are shown in Figure 6.8. A bigger spread is visible above 50 Hz.

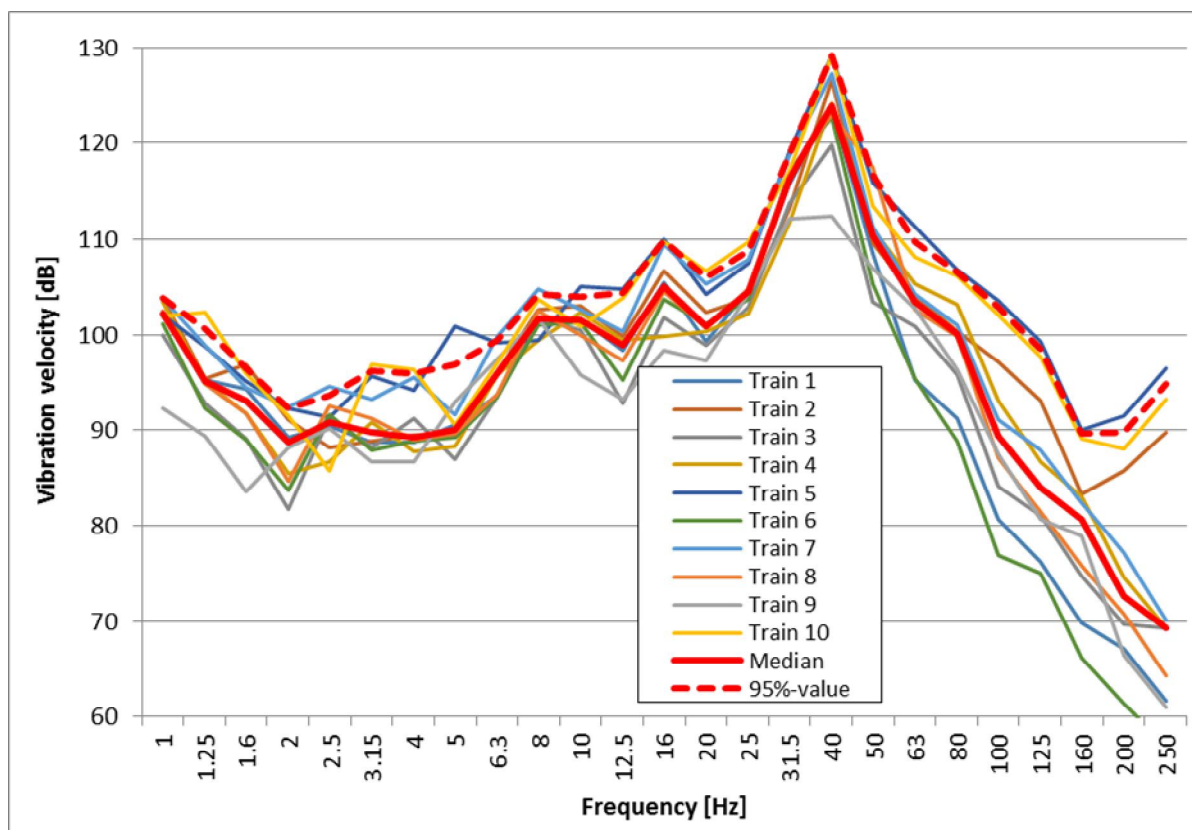


Figure 6.8: Measurements in Furet for test sheet piling wall (before installing) 10 passenger train X31 at speed 77 km/h \pm 5%, at 8 m distance.

In Figure 6.9 the measurements of the reference site in Furet after the tamping are shown for 11 freight trains at speed 43 km/h \pm 6% at 8 m distance. A bigger spread is visible at 50 Hz and lower frequencies.

Figure 6.10 shows the difference of the 95%-percentile value of these train measurements to the median value. Normally a difference over a factor of 6 dB (Factor of 2) is visible for freight trains. For Intercity trains at 50 Hz differences of 6 dB and higher are visible.

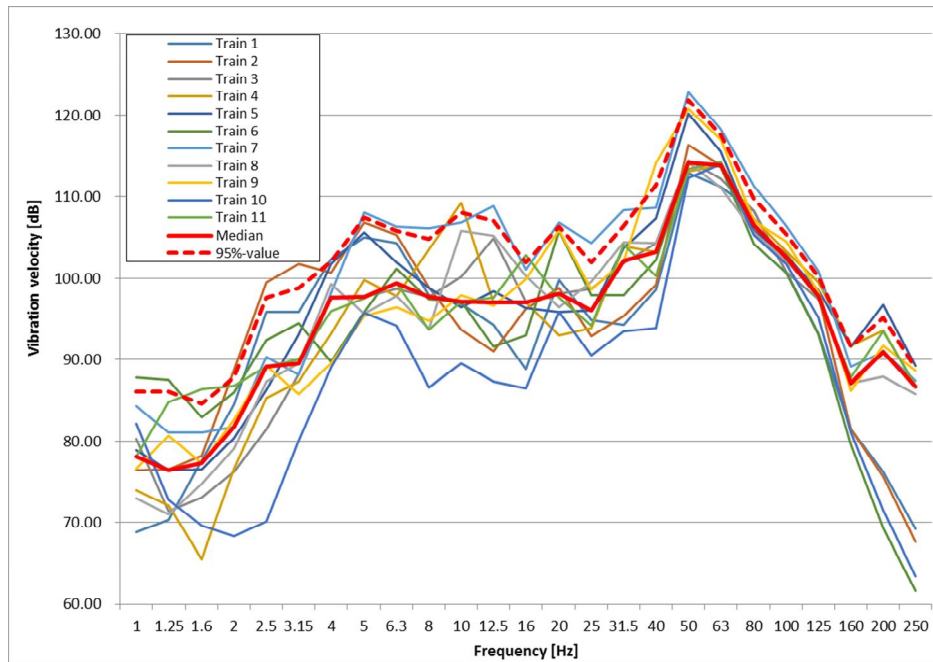


Figure 6.9: Reference site Furet for tamping with low track defects. 13 freight trains at speed 43 km/h \pm 6%, at 8 m distance

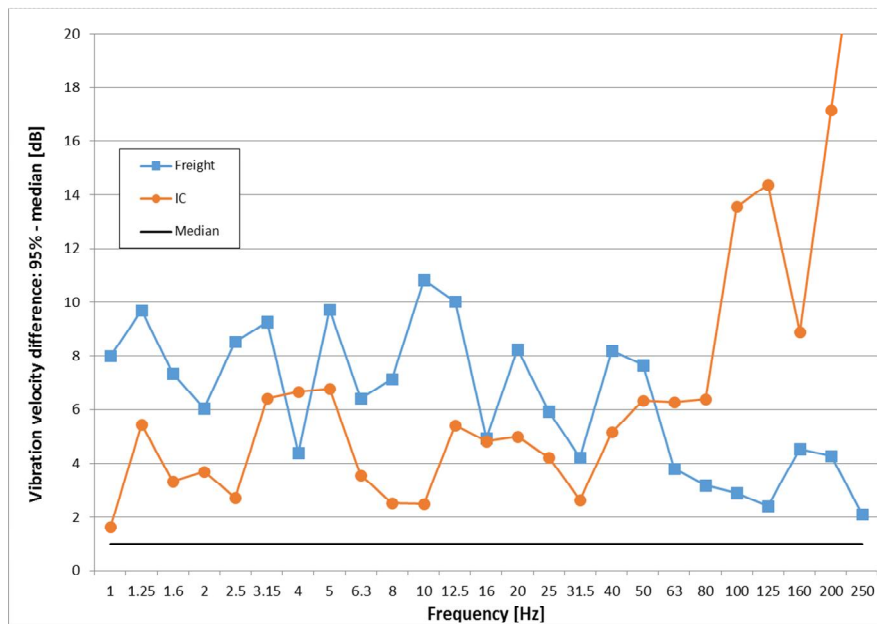


Figure 6.10: Difference of emission spectra (95%-percentile – median value) for two Swedish measurement campaigns: Reference situation for a) freight traffic for test track maintenance in Furet and b) IC trains for test sheet piling wall in Furet.

6.2 FURTHER RIVAS MEASUREMENTS IN SWITZERLAND

For deliverable D2.2 [1] and D5.4 [2] a big analysis on train measurements (every bogie is analysed separately) was performed in Switzerland at the locations Thun, Ligerz and Cadenazzo. A short analysis on some results is shown in this Section.

6.2.1 Measurements in Thun

Figure 6.11 illustrates the results in Thun for 8 m distance for different wagon types with 60-70 km/h. The freight locomotives show especially high values for the median and 95%-percentile, see lower and upper value of the rectangles.

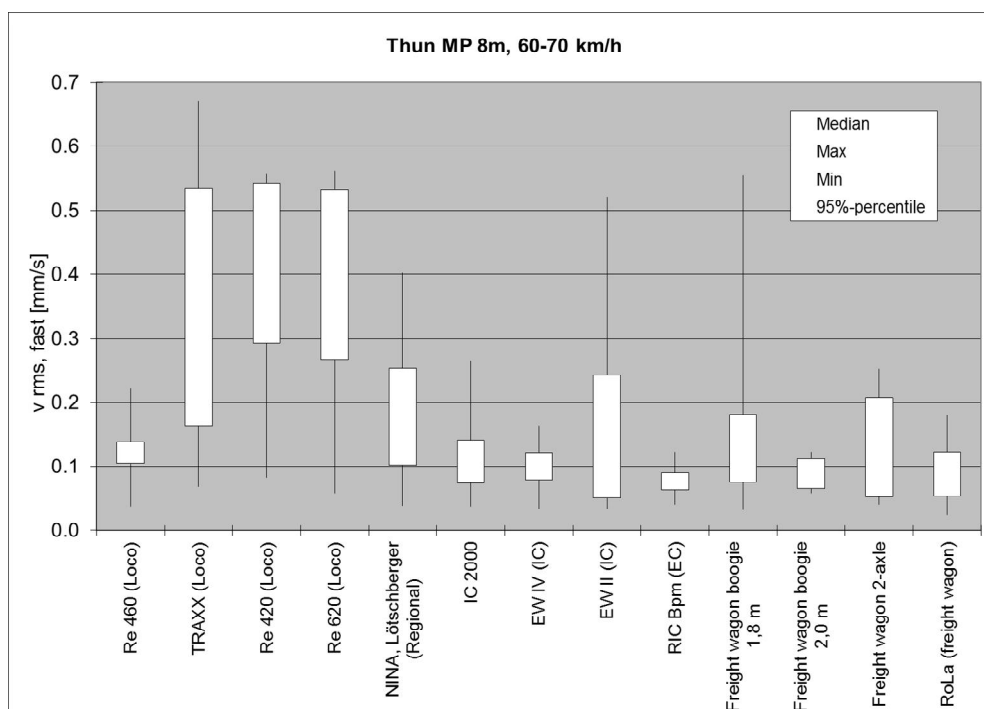


Figure 6.11: Measurements of V_{rmsmax} in Thun, 8 m distance, for different train types (60-70 km/h).

Figure 6.12 contains the frequency analysis of these measurements. The TRAXX locomotive Re482/Re484 as well as the regional train Nina show respectable vibration values below the freight locomotives Re420 and Re620.

Figure 6.13 shows for the freight wagon with Y25 (1.8 m axle distance) between 50-125 Hz around a factor of 4 by comparing 95%-percentile and median value. This indicates a high potential of relevant mitigation effect for maintenance. There is less potential for passenger wagons.

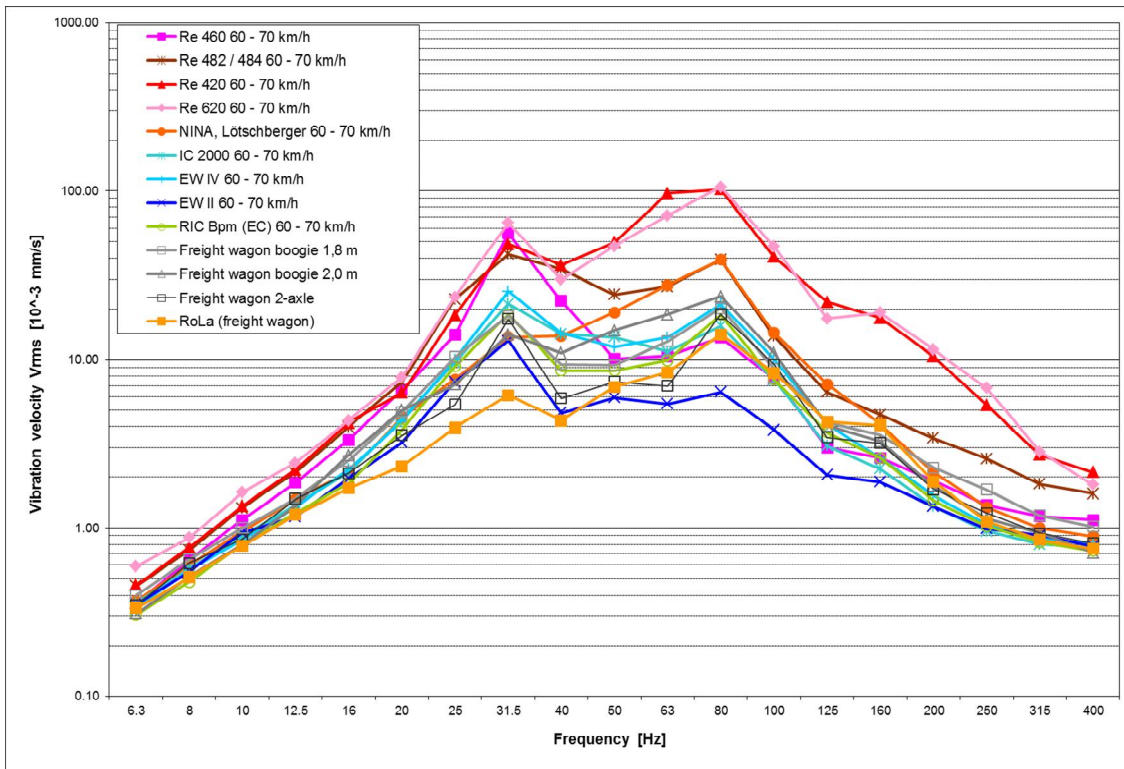


Figure 6.12: Frequency analysis of measurements Thun (60-70 km/h), median for 8 m distance.

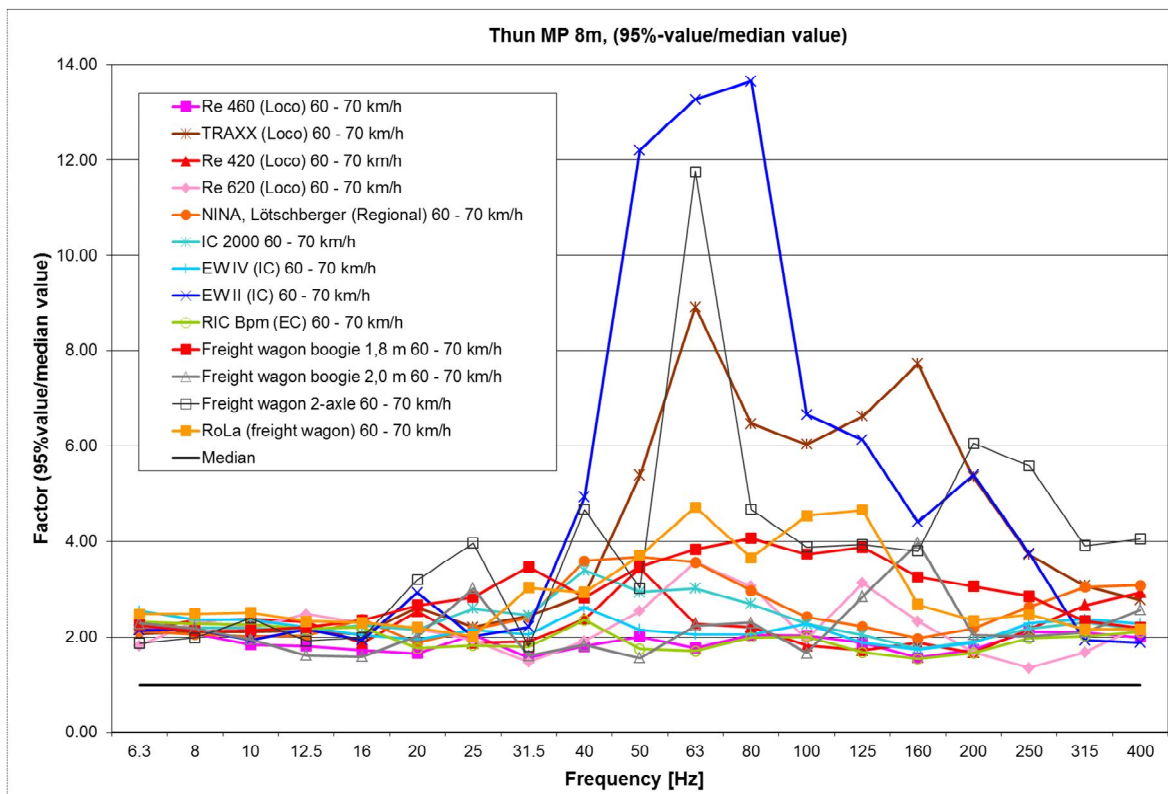


Figure 6.13: Factor 95%-value/median of measurements Thun (60-70 km/h), 8 m distance.

6.2.2 Measurements in Ligerz

Figure 6.14 illustrates the results in Ligerz for 8 m distance for different wagon types with 70-80 km/h. The Domino with accelerated wheels show especially high values for the 95%-percentile, see upper value of the rectangles. The freight locomotives have high median values.

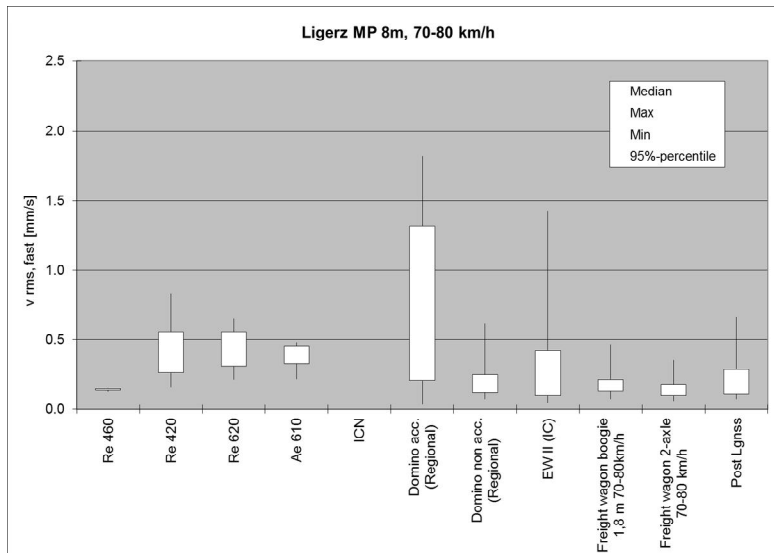


Figure 6.14: Measurements of V_{rmsmax} in Thun, 8 m distance, for different train types (60-70 km/h).

Figure 6.15 illustrates the results in Ligerz in 8 m distance for different wagon types with 70-80 km/h. The freight locomotives show high vibration values (Re420, Re620, Ae610) but also the regional Domino wagon with driven wheelsets, similar to the results in Brunnen. Figure 6.15 shows especially for the Domino with accelerated wheels significant differences comparing 95%-percentile and median value. This indicates a high potential of relevant mitigation effect for maintenance. It seems that here is less potential for freight wagons for Frequencies below 100 Hz.

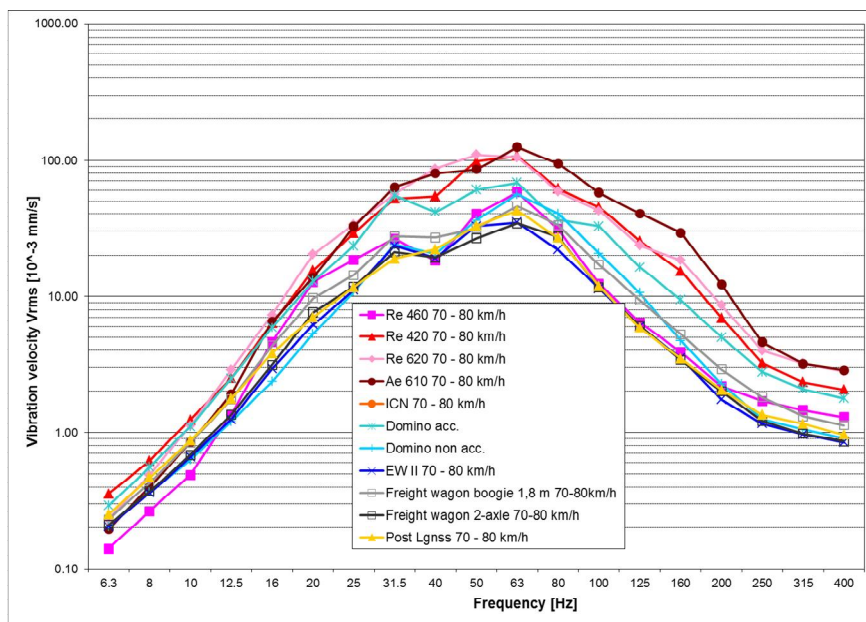


Figure 6.15: Frequency analysis of measurements Ligerz (70-80 km/h), median at 8 m distance.

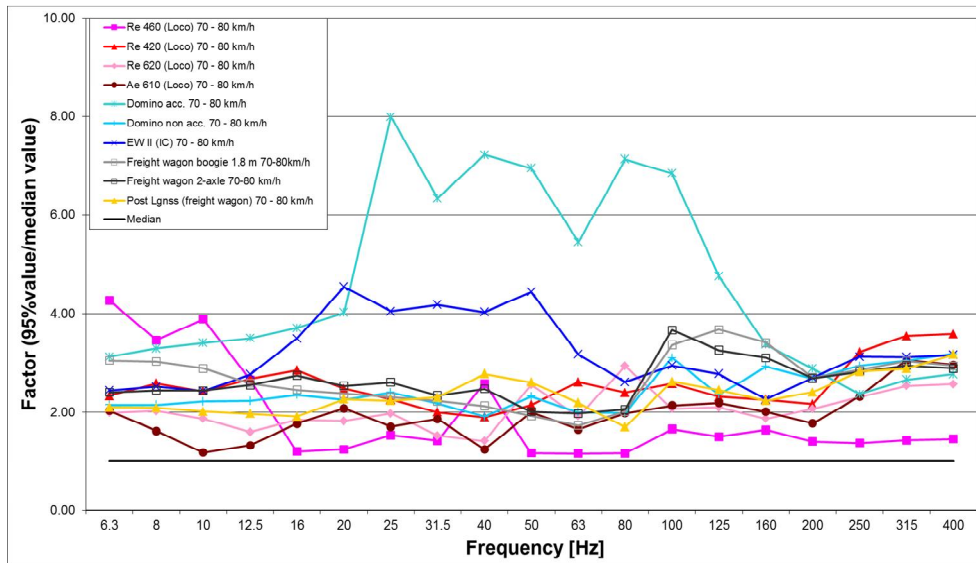


Figure 6.16: Factor 95%-value/median of measurements Ligerz (70-80 km/h), 8 m distance.

6.2.3 Measurements in Cadenazzo

Figure 6.17 illustrates the results in Ligerz for 8 m distance for different wagon types with 70-80 km/h. The Domino with accelerated wheels show especially high values for the 95%-percentile, see upper value of the rectangles. The freight locomotives have high median values.

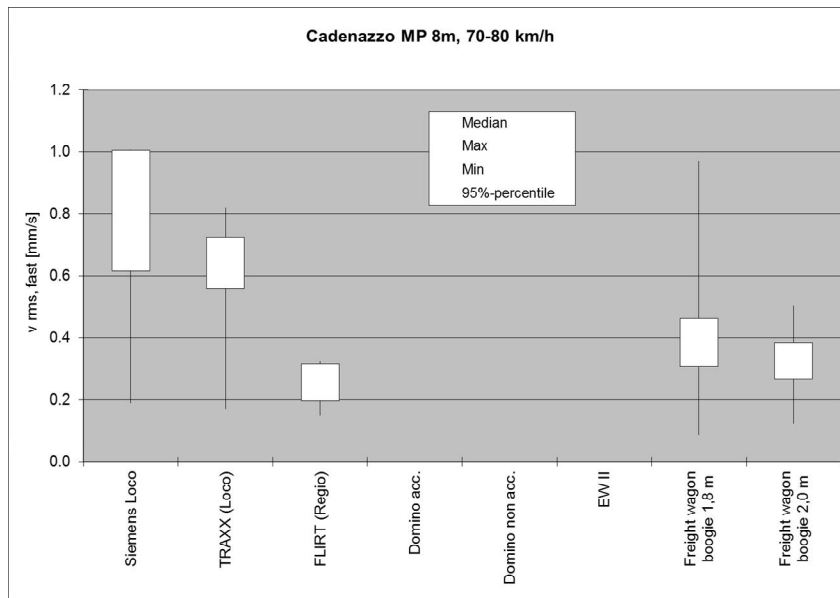


Figure 6.17: Measurements of V_{rmsmax} in Cadenazzo, 8 m distance, for train types (70-80 km/h).

Figure 6.18 illustrates the results in Cadenazzo in 8 m distance for different wagon types with 70-80 km/h. The modern freight locomotives show high vibration values (Siemens and TRAXX). Figure

6.19 shows for no train type significant differences comparing 95%-percentile and median value. This indicates a lower potential to solve problems by maintenance.

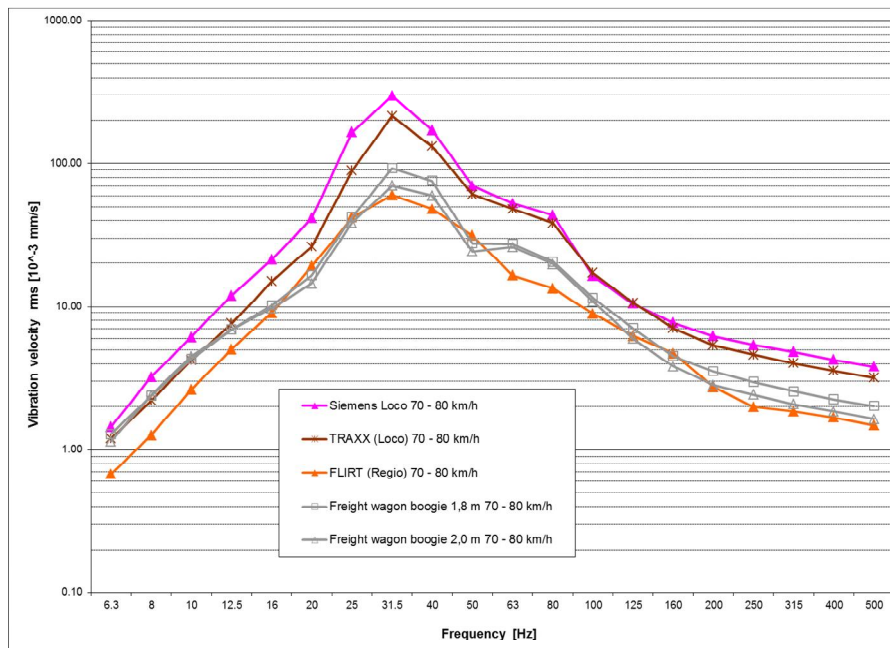


Figure 6.18: Frequency analysis of measurements Ligerz (70-80 km/h), median at 8 m distance.

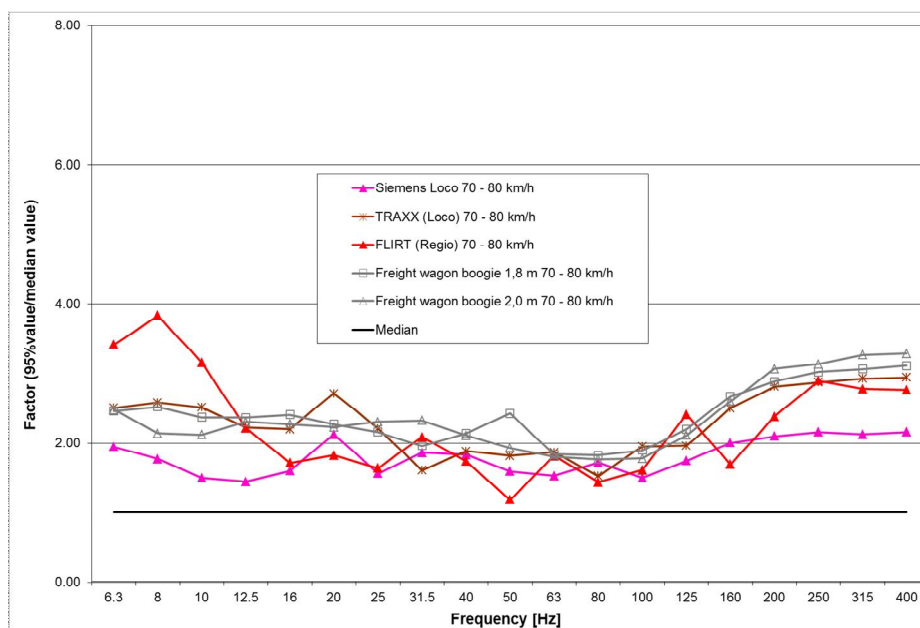


Figure 6.19: Factor 95%-value/median of measurements Ligerz (70-80 km/h), at 8 m distance.

6.2.4 Comparison of the three sites

An overall analysis of Vrmsmax (median as well as 95%-percentile) is shown in Table 6.2 for the three measurement sites Thun, Ligerz and Cadenazzo. Values over a factor of 2 (95%/median and max/95%) are in bold. It is visible that the freight wagon with Y25 (1.8 m axle distance) shows for

all 3 sites more than a factor of 2 especially for the factor max/95%. This indicates that a small percentage of freight wagons gives extremely high vibration values.

Wagon type	Thun 60-70 km/h					Ligerz 70-80 km/h					Cadenazzo 70-80 km/h				
	median	95%	max	95%/median	max/95%	median	95%	max	95%/median	max/95%	median	95%	max	95%/median	max/95%
Re 460 (Loco)	0.107	0.142	0.163	1.332	1.147	0.138	0.150	0.151	1.085	1.008					
TRAXX (Freight Loco)	0.135	0.368	0.656	2.727	1.784						0.558	0.727	0.818	1.302	1.128
Siemens (Freight Loco)											0.614	1.004	1.007	1.635	1.003
Re 420 (Freight Loco)	0.198	0.346	0.386	1.743	1.118	0.267	0.558	0.831	2.090	1.489					
Re 620 (Freight Loco)	0.214	0.344	0.437	1.605	1.269	0.313	0.557	0.652	1.780	1.170					
NINA, Löscherberger (Regional)	0.074	0.162	0.247	2.199	1.529										
Domino acc. (Regional)						0.211	1.318	1.821	6.253	1.382					
Domino non acc. (Regional)						0.122	0.250	0.619	2.054	2.472					
FLIRT (Regional)											0.197	0.316	0.325	1.601	1.031
IC 2000	0.070	0.118	0.203	1.684	1.725										
EW IV (IC)	0.073	0.106	0.143	1.457	1.347										
EW II (IC)	0.053	0.162	0.392	3.026	2.426	0.099	0.424	1.426	4.296	3.359					
RIC Bpm (EC)	0.056	0.087	0.107	1.547	1.221										
Freight wagon boogie 1.8 m	0.071	0.165	0.410	2.330	2.485	0.132	0.218	0.466	1.649	2.134	0.307	0.463	0.971	1.508	2.098
Freight wagon boogie 2.0 m	0.064	0.100	0.107	1.570	1.069						0.266	0.385	0.504	1.446	1.309
Freight wagon 2-axle	0.056	0.165	0.189	2.923	1.148	0.102	0.184	0.355	1.806	1.930					
RoLa (freight wagon)	0.051	0.100	0.132	1.963	1.325										
Post Lgnss (freight wagon)						0.110	0.289	0.664	2.618	2.296					

Table 6.2: Table of Vrmsmax as median, 95%-percentile, maximum value and proportionality of 95%-percentile/median and max/95%-percentile, at 8 m distance.

Figure 6.20 compares the freight wagons with Y25 (1.8 m axle distance) for the three sites. The distribution for this wagon type seems to be site dependent but so far the reason for these differences is unclear but also for the Vrmsmax, Thun in Table 6.2, shows the highest values as in Figure 6.20.

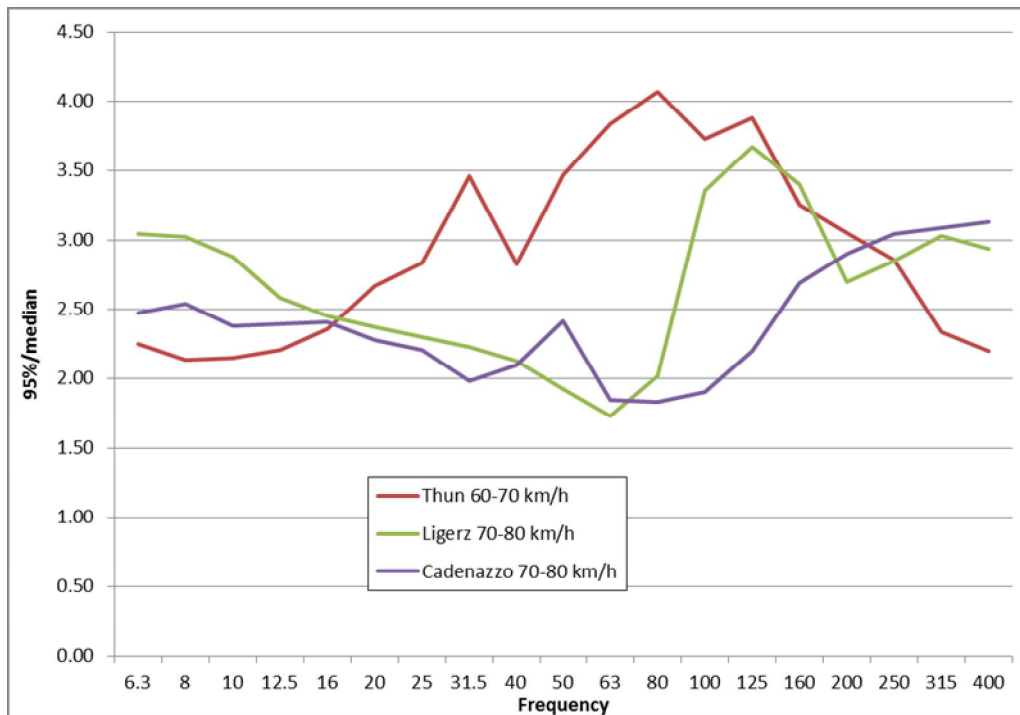


Figure 6.20: Proportionality of 95%-percentile and median value of Y25 freight bogie at different sites at 8 m distance.

6.3 CONCLUSIONS

The statistical distribution show for some of the vehicle types a good potential to reduce vibration excitation by maintenance. The freight wagon with Y25 (1.8 m axle distance) shows for all 3 Swiss sites a potential reduction by more than a factor of 2 especially when looking at the factor of maximum values divided by 95%-percentile. This indicates that a small percentage of freight wagons gives extremely high vibration levels and that if these freight wagons could be maintained the maximum value could decrease by around 6 dB.

The Swedish measurements are analysed differently (whole train passage). Just little more scattering for freight than for Intercity trains is seen.

7. LIFE CYCLE COST ANALYSIS

The dynamic component of vertical wheel-rail contact forces generated by wheel irregularities (wheel out-of-roundness) is an important source to ground vibration and ground-borne noise. To reduce this kind of environmental disturbance wheelsets require regular attention on a wheel lathe to remove tread defects and to restore excessive deviation of the tread profile from the nominal standard profile due to wear. Fact is that railway vehicles are still in operation causing significant environmental impact. This signifies that there is a gap in wheelset maintenance and therefore changes of wheel maintenance process are required. From the viewpoint of management, however, additional maintenance costs arise there without getting anything in return. This is not taking into account that the environmental impact is a result of excessive damage to the wheel treads. This damage affects not only the environment but also cause costly damages to the vehicles and the infrastructure. The present Chapter (see also [7]) is therefore intended to provide a basis for economic considerations in the wheelsets and their maintenance.

7.1 SCOPE AND METHODOLOGY FOR THE ASSESSMENT

Deliverable D2.7 [4] reported that the costs for wheelset maintenance, apart from costs of vehicle operating loss, depend predominantly from the wheel replacement costs (including the procurement costs for new wheels). On long term this costs can be influenced in a limited range by optimised maintenance. In this report, a simple method will show what the maintenance costs depend on and how they can be influenced. The costs will be calculated on basis of the durability diagrams in [8] and the costs for restoring wheel profiles on lathes at SBB and wheel replacement in SBB workshops.

7.2 UNDERSTANDING TREAD DEFECTS OF SBB LOCOMOTIVE RE 420

7.2.1 Determinant faults causing reprofiling on locomotives Re420

The determinant faults causing reprofiling on locomotives Re420 is tread wear and rolling contact fatigue (RCF). Flange wear is not critical (around 1 mm flange wear for 100'000 km) due to efficient on board flange lubrication. According to Figure 7.1, flange wear would cause a reprofiling depth of 2.5 mm per 100'000 km or a diameter reduction of 5 mm/100'000km. As can be seen later, the reprofiling depth is much higher than the depth required to restore the profile. Tread wear expressed in flange height rate per 100'000 km is between 2 mm and 2.5 mm (diameter reduction between 4 and 5 mm) depending of

- operating conditions (line characteristics, applied traction and braking forces...),
- wheel material characteristics.

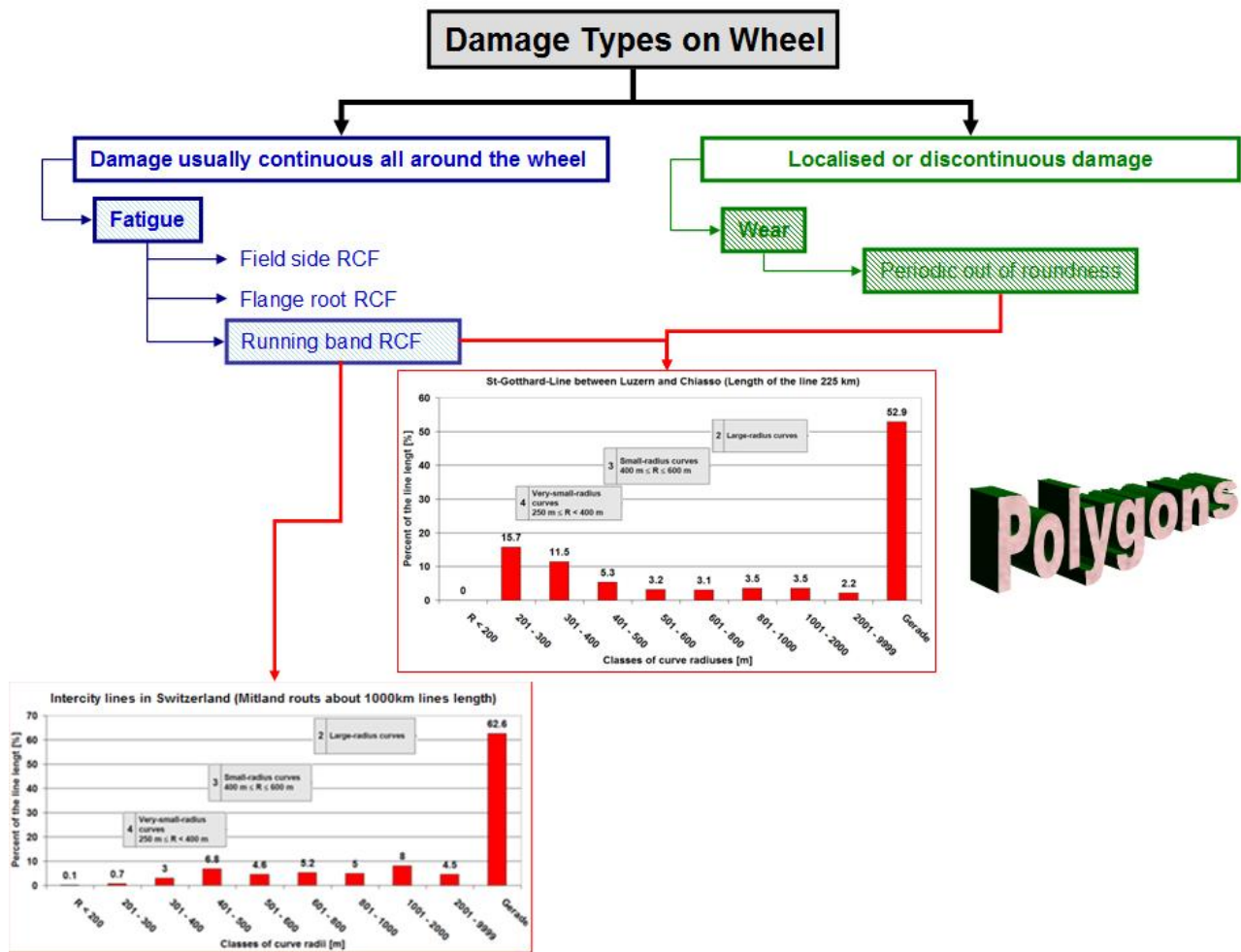


Figure 7.1: Wheel tread damage types on locomotives Re420

Faults causing reprofiling of locomotives Re420 depend on the line characteristics. The first characterisation defined by the curve distribution on the left side in Figure 7.1 provokes determinant faults causing reprofiling of the type “running band RCF”. The second characterisation defined by the curve distribution on the right side in the Figure 7.1 provokes determinant faults causing reprofiling of the type “periodic out of roundness” accompanied with “running band RCF”.

Figures 7.2 and 7.3 show typical RCF faults on wheel treads of locomotives Re420. The faults are located in the running band. The orientation of the cracks (see picture on the right in Figure 7.2) is in the horizontal direction. That means that the mechanism for crack propagation is based on longitudinal creep forces.

Wheel tread before grinding



Wheel tread after grinding



Detail showing crack orientation



Figure 7.2: RCF damage before and after grinding (on the right detail of RCF crack orientation visible after grinding)

RCF in running band of Re420



Figure 7.3: RCF in running band of locomotive Re420

Based on test results of SBB a cut of around 6 mm depth (diameter reduction of around 12 mm) is needed to remove the RCF cracks.

7.2.2 Contact patch wheel/rail

When running on a straight track or on lines with very large curve radii contact patches of all vehicle wheels will be situated around the running band (centre of the wheel tread).

Figure 7.4 shows the positions of leading and trailing wheelsets of a two-axle bogie when running in right-hand 500 m-curve with a lateral acceleration on track level of 0.8 m/s^2 . Figure 7.5 shows the correspondent contact points of the four wheels.

The rolling line of the leading wheelset is displaced around 7 mm out of track centre in the direction of outside curve. The contact patch of the outer wheel (left wheel) is situated in the flange root band (see Figure 7.5). The contact patch of the inner wheel (right wheel) is situated in the so called RCF-band (field side band see Figure 7.5). On the wheel treads of the locomotive Re420 there are visible little cracks in these contact areas, but cavities do not occur. This signifies that elevated creep forces wear away RCF in these areas (product of T-gamma, see [9]). The rolling line of the trailing wheelset is displaced 0.24 mm out of track centre in the direction of outside curve. The contact patches of the two wheels are situated in the circumstances of the rolling band (see Figure 7.5). On the wheel treads of the locomotives Re420 RCF occurs in this contact areas (see Figures 7.2 and 7.3). This means that crack propagation on locomotives of type Re 420 occur only in this area. On the other areas, initiated cracks will be worn away.

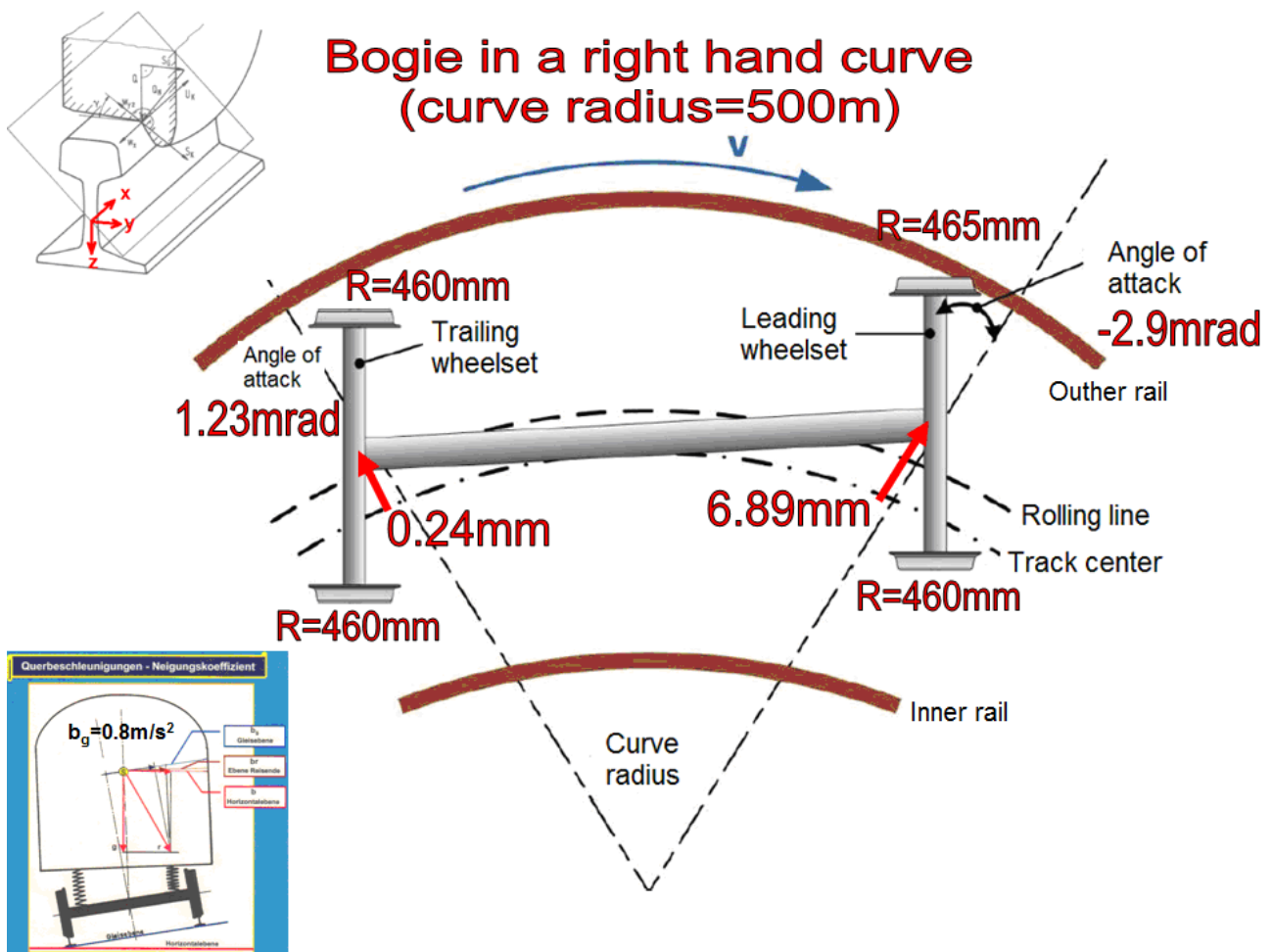


Figure 7.4: Sketch of positions of wheelsets of a two-axle bogie when running in a curve

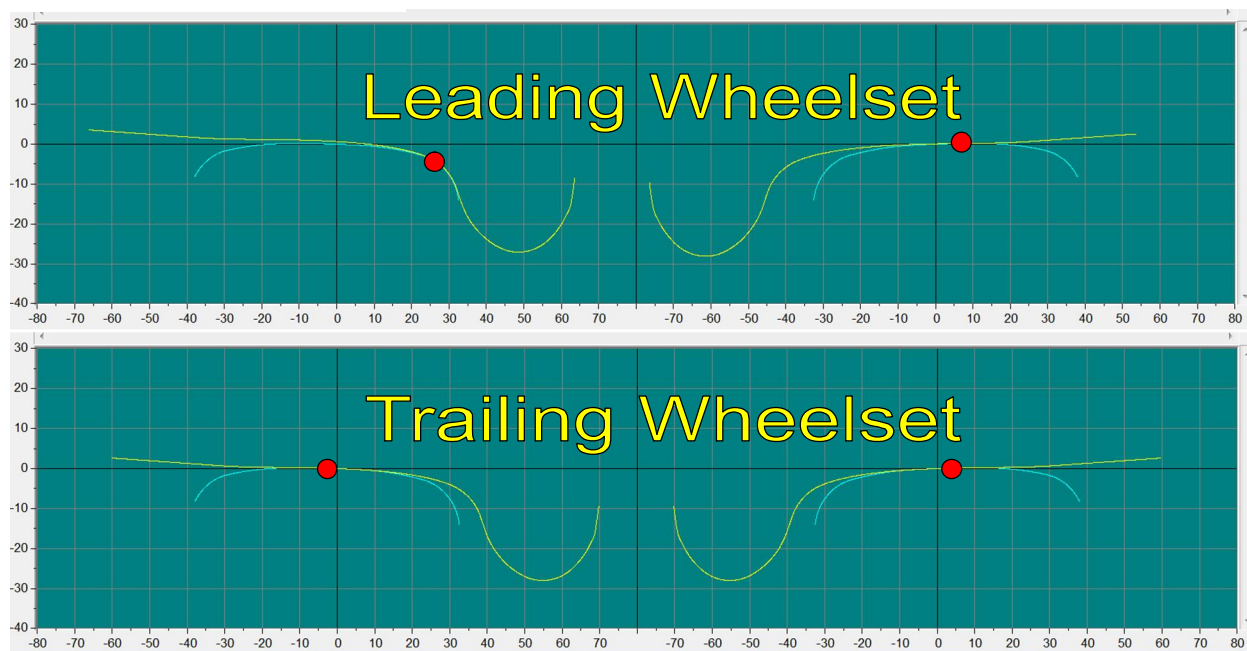


Figure 7.5: Contact points on wheels of leading and trailing wheelsets (positions of wheelsets according to Figure 7.4)

7.2.3 Crack propagation

In fracture mechanics there are two fundamental mechanisms. The first one concerns crack initiation and the second one concerns crack propagation. Crack initiation has been explained by Shake-down theory (see for example [10]). Crack propagation and damage patterns are discussed for example in [11] and [12]. Figure 7.6 illustrates the mechanisms of crack propagation. Cracks on rails in curves (head checks) are mostly observed in the contact pattern of the outer rail. Cracks on trailer wheels are mostly observed in the contact pattern of the inner wheel. The two crack bands are illustrated on the right side of Figure 7.6. The mechanism of crack propagation is based on the facts that

- cracks will be opened by driving forces before entering in the contact patch,
- the crack will be closed by the contact forces when the opened crack enters in the contact patch,
- if fluid is present (humidity or water) this fluid will enter into the opened crack and when the crack is closed by the contact forces additional hydrostatic pressure will be produced and as a consequence the crack propagates.

This mechanism of crack propagation shows that the crack has to be opened (by driving forces) *before* the crack is entering in the contact pattern so that the crack can propagate. As can be seen in Figure 7.6, as an example for a leading wheelset in a right hand curve, cracks will be

- closed by the creep forces on the outer wheel before entering into the contact patch,
- opened by the creep forces on the inner wheel before entering into the contact patch.

The opposite happens for the rail. Based on this model, crack propagation is only possible if the tangential forces open the crack before entering into the contact patch. This signifies for the wheel that crack propagation is only possible if the tangential forces are acting in the opposite direction of the trains driving direction (operating direction). Based on this fact, crack propagation in Figure 7.6

is only possible at the inner wheel of the leading wheelset and at the outer wheel of the trailing wheelset. The yellow arrows in Figure 7.6 show the direction of forces acting when traction or braking forces are applied. Traction forces tend to close the cracks before entering into the contact patch and braking forces tend to open them. For the rail, the opposite is valid.

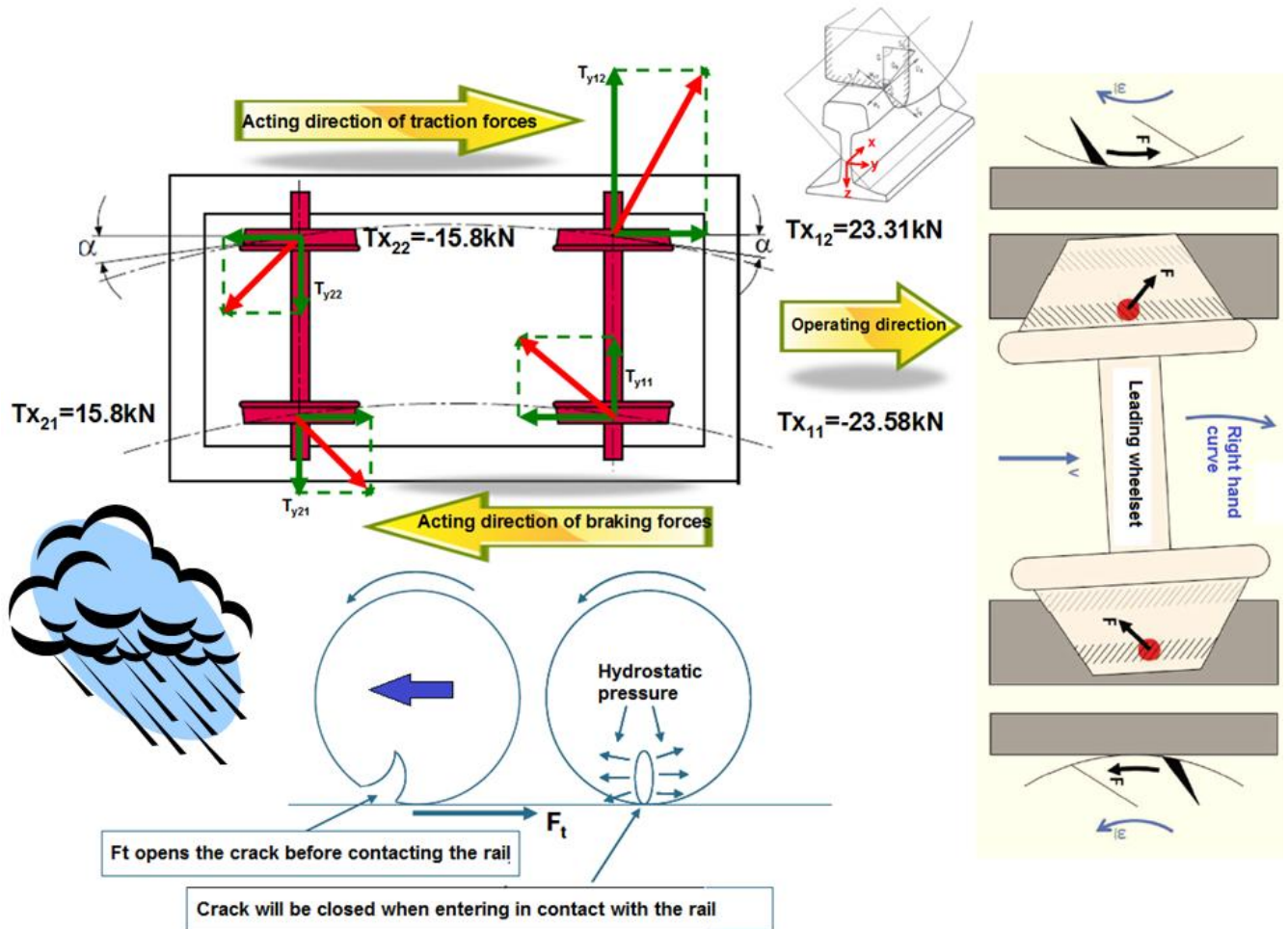


Figure 7.6: Crack propagation in wheels and rails contact pattern

Figure 7.7 shows the influence of braking and traction forces on the direction of the creep forces. The calculations are carried out for a locomotive in a narrow right hand curve with a speed corresponding to a lateral acceleration on track level of -0.3 m/s^2 . On the top of the figure the creep forces without traction or braking forces are presented. If traction forces are overlapped, the tangential forces of all wheels are vectored in the operating direction. In this case, there is no crack propagation on the wheel. If braking forces are overlapped, the tangential forces of all wheels are vectored inverse to the operating direction. In this case, there is a risk of crack propagation on all wheels.

Figure 7.8 shows the tangential forces for a locomotive running without braking or traction forces in a 300 m curve. The speed is in accordance with a non-compensated lateral acceleration on track level of 0.8 m/s^2 . In addition to the creep forces, also the T-gamma values are represented. It can be seen that

- on the leading wheelset the dominating mechanism is wear,
- on the trailing wheelset the dominating mechanism is RCF.

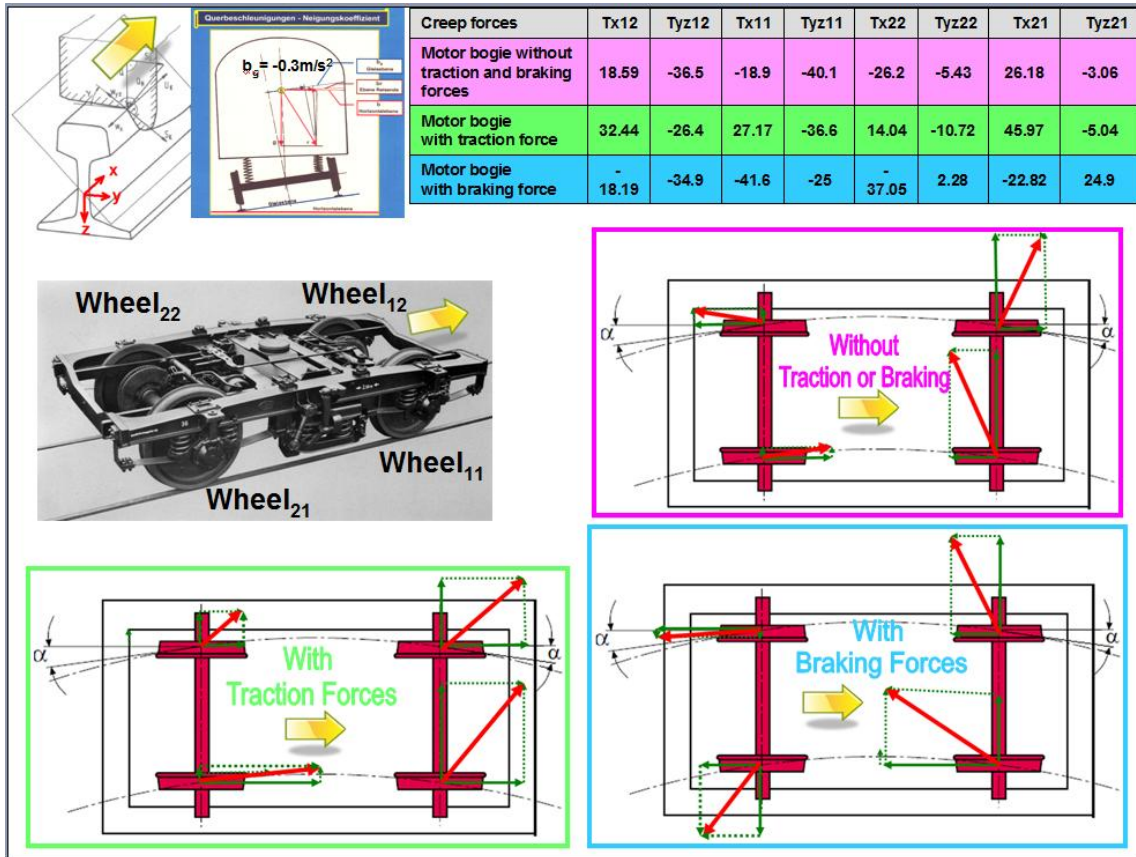


Figure 7.7: Influence of traction and braking forces on the direction of creep forces

Locomotive travelling in a 300m curve (without traction and braking forces)

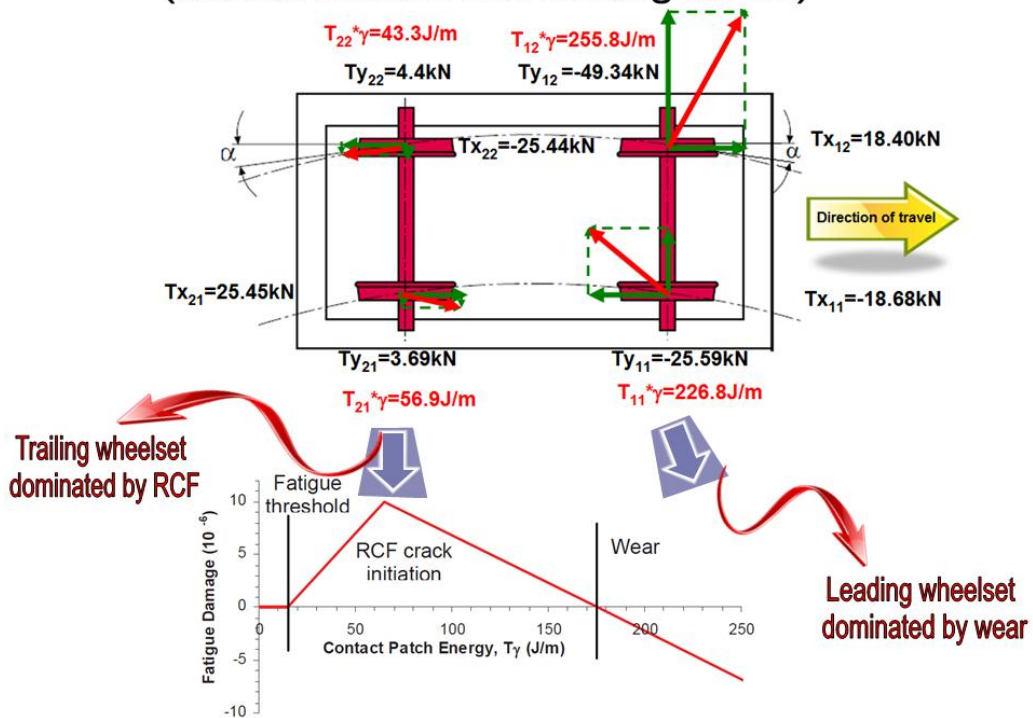


Figure 7.8: Locomotive travelling in a 300m curve without traction and braking forces

7.2.4 Damage mechanisms on locomotive Re 420

The wheel damage relationship is more difficult than the corresponding rail damage relationship. A rail is installed as either a high or low rail on a given curve radius and usually experience fairly consistent traffic (vehicle types, direction, speed and traction/braking). Consequently, the damage mechanisms on a length of rail are consistent. However, a wheel runs in both directions, experiences a wide range of curve radii (on both left and right hand curves) and traction as well as braking forces. All the damage from these different running conditions is superimposed on the wheel tread and cannot easily be related to specific route sections or running conditions. The overall damage rates on the wheel are therefore much more sensitive to the relative rates of wear and crack growth.

Based on the above explanations it must be assumed that the damage mechanisms for the locomotives Re420 are

- wear on the leading wheelsets (polygonisation is a consequence of wear in narrow curves),
- RCF on the trailing wheelsets.

In addition, it must be considered that the locomotive Re420 applies a powerful electrodynamic brake which implies that the wheels of Re420 are quite stressed and more crack propagation is possible.

7.3 LCC CALCULATION FOR SBB LOCOMOTIVE RE 420

7.3.1 Input parameters

Based on durability diagrams the wheelset maintenance costs can be estimated as follows [4]:

Total costs for Time T ($C_{Time T}$) =

$$N_1 * (C_{\text{Reprofiling}} + C_{\text{Operation loss reprofiling}} + C_{\text{Transfer vehicles to Wheel lathe}}) + N_2 * (C_{\text{Wheel Replacement}} + C_{\text{Operation loss wheel replacement}} + C_{\text{Transfer vehicles to overhaul workshop}})$$

where N_1 : Quantity of reprofiling, N_2 : Quantity of wheel replacements, C:Costs

The cost for periodic controls of the wheel treads and the wheelsets as well as the costs for the spare parts storing are not included in the above formula.

If in time T the vehicle travels X kilometres, the specific costs are

$$T_{\text{specific per kilometer}} = \frac{C_{Time T}}{X} \left[\frac{\text{Euro}}{\text{Kilometer}} \right]$$

The durability diagrams utilized for the calculations derive from [8]. Figure 7.9 shows the durability diagram established during the investigations carried out in [8] for two different well defined steel qualities (“B4N”, “Exzellent”) for the wheel tyres of the locomotive Re420. The diagrams show

- a lower wear rate of steel quality “Exzellent” ($\Delta D \approx 4$ mm/100'000 km) compared to steel quality “B4N” ($\Delta D \approx 5$ mm/100'000 km),
- a longer reprofiling interval for steel quality “Exzellent” (154523 km) compared to steel quality “B4N” (121551 km),
- a lower cut for reprofiling for steel quality “Exzellent” ($\Delta D = 11.69$ mm) compared to steel quality “B4N” ($\Delta D = 12.4$ mm),
- a higher interval for wheel replacement for steel quality “Exzellent” (611'000 km) compared to steel quality B4N (460'000 km).

Costs for reprofiling wheels on an under floor lathe, for wheel replacement and for operation losses per day within the SBB were be taken into account for the following LCC-analysis in this chapter. The costs for vehicle transfer have not been considered. The costs for preventive maintenance (wheel control and monitoring) have not been considered, because there are other reasons determining the maintenance intervals (changing of brake shoes, control of bogie frame and suspensions, filling up recipients for sanding and flange lubrication, ...).

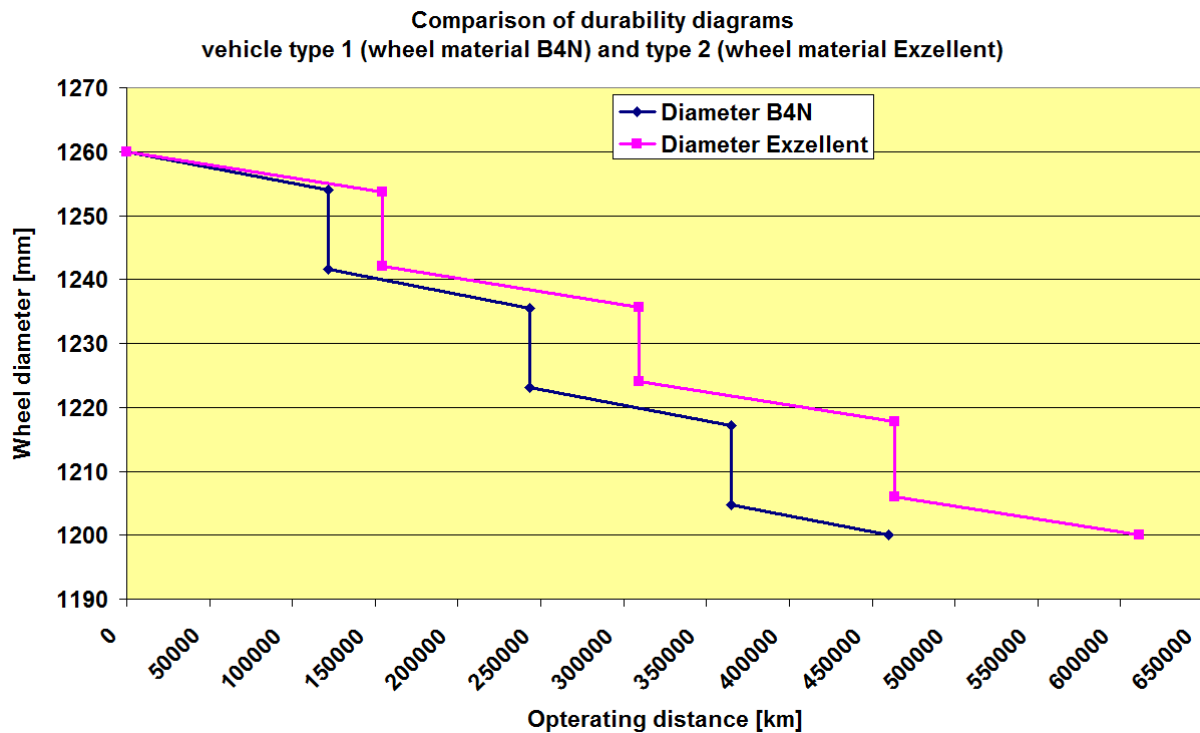


Figure 7.9: Durability diagrams for Re420 with steel qualities type 1 and type 2

7.3.2 Costs for reprofiling

Figure 7.10 shows the costs per km for reprofiling in dependence of the operating distance since the last reprofiling. One curve contains the costs for reprofiling only and the other curve contains the costs for reprofiling including the operation loss due to the vehicle immobilisation. It can be seen that costs for vehicle immobilisation influence considerably the reprofiling costs. On the other side it can be seen that due to the hyperbolic course of the function there is big influence of reprofiling intervals on costs at lower reprofiling intervals. At higher reprofiling intervals the relation between costs per kilometer and operating distance are less sensitive.

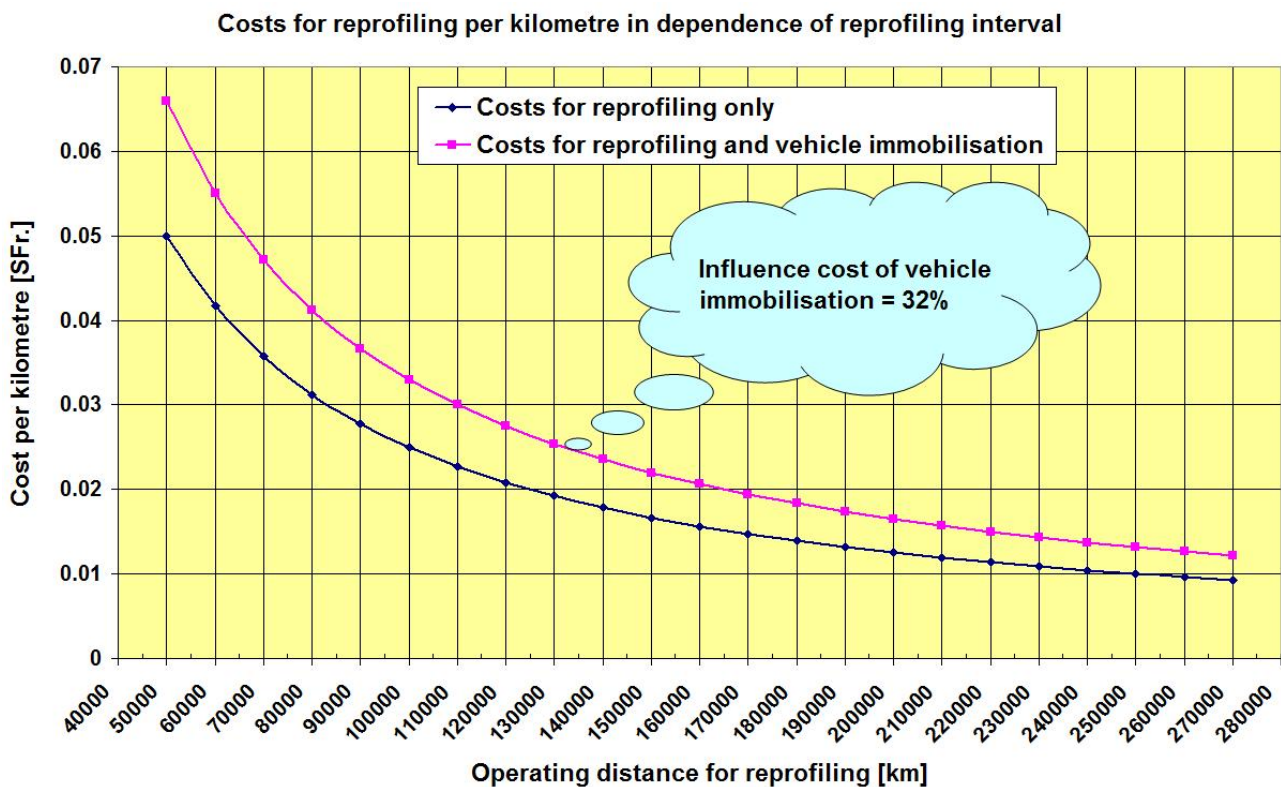


Figure 7.10: Costs per kilometre for reprefiling in dependence of reprefiling interval

7.3.3 Costs for wheel replacements

Figure 7.11 shows the costs for wheel replacement in function of the operating distance. One curve contains the costs for replacement only and the other one including the costs for vehicle immobilisation. It can be seen that costs for vehicle immobilisation do only marginally influence the wheel replacement costs. On the other side it can be seen that due to the hyperbolic course of the function there is big influence of wheel replacement intervals on costs at lower replacement intervals. At higher wheel replacement intervals the relation between costs per kilometre and operating distance are less sensitive.

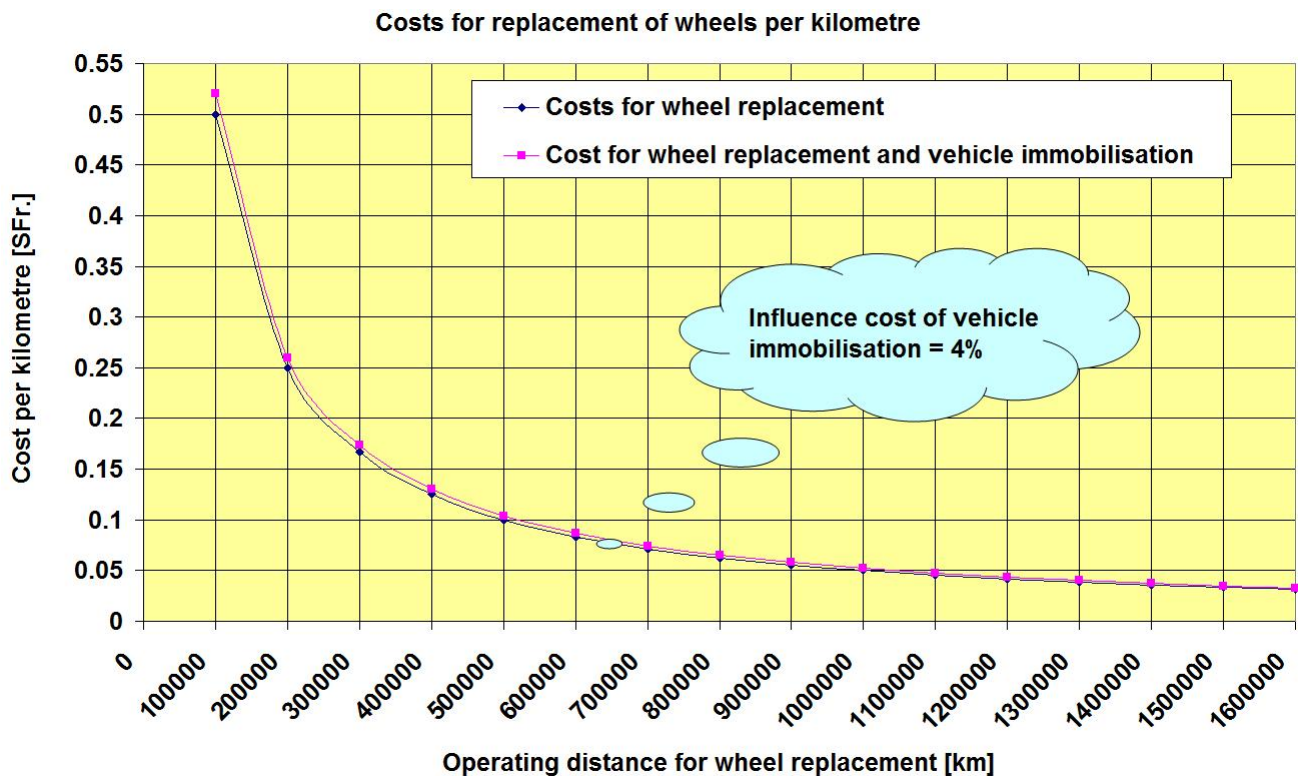


Figure 7.11: Costs per kilometre for wheel replacement in dependence of reprofiling interval

7.3.4 Durability diagrams and costs

Figures 7.12 and 7.13 shows the durability diagrams and costs for the two different wheel materials. It can be seen that the costs are the same for both steel qualities. The difference is that the costs are incurred for different mileages. For this reason, the costs per unit of the mileage are different. This is represented in Figure 7.14. By augmenting the wear resistance and the resistance to RCF of the wheel material in the present case results a reduction of cost per kilometre of SFr. 0.03 or of around 25%.

Figure 7.15 shows on the top the cost distribution for reprofiling and wheel replacement. For both steel qualities, there are attributed 16% for reprofiling and 84% for wheel replacement. The same amount of allocation for the both steel qualities is due to the fact that there are the same quantities of reprofiling between wheel replacements for both steel qualities. The difference in costs is due to the fact that steel quality Exzellent dispose over a longer lifetime (expressed in kilometres') than the steel quality B4N. On the other side the diagrams below show that for both steel qualities the diameter reduction due to reprofiling is more important than that one for abrasive wear. Due to the fact that the diameter reduction by reprofiling is a consequence of RCF, a considerable improvement in LCC can be achieved by the application of steel qualities that are more resistant to RCF.

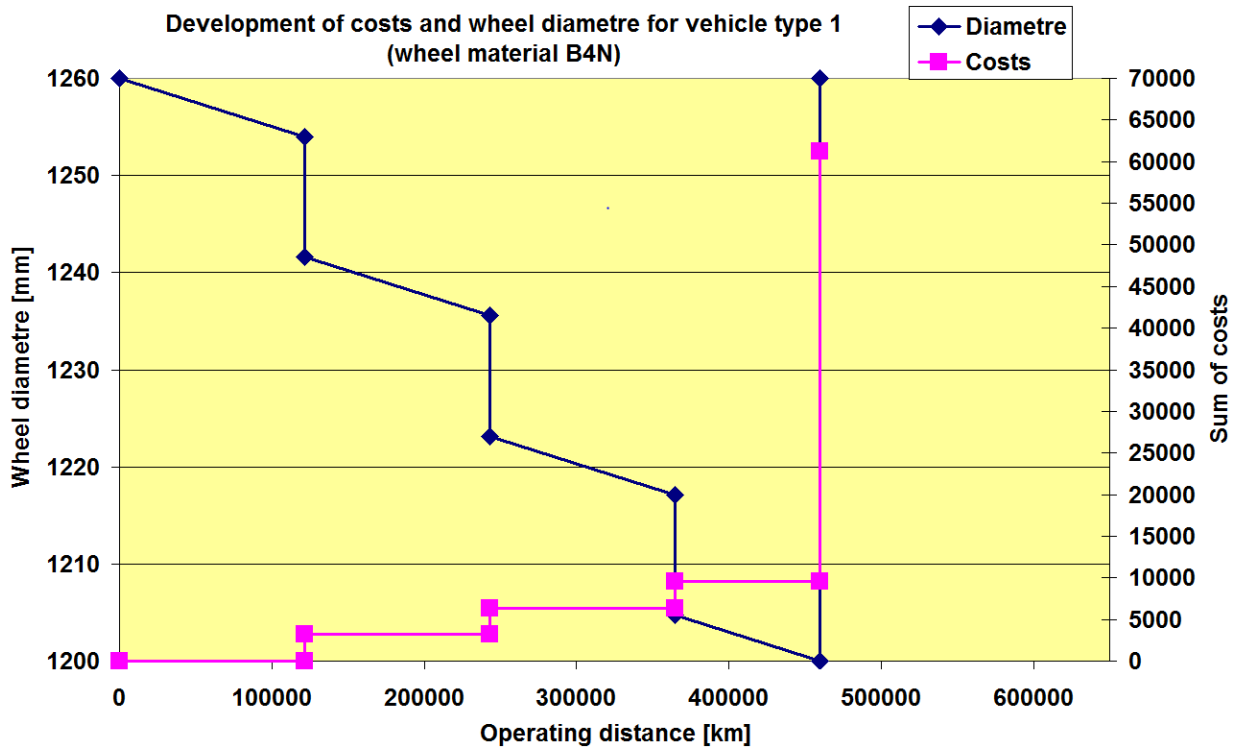


Figure 7.12: Durability diagram and costs for wheel material B4N

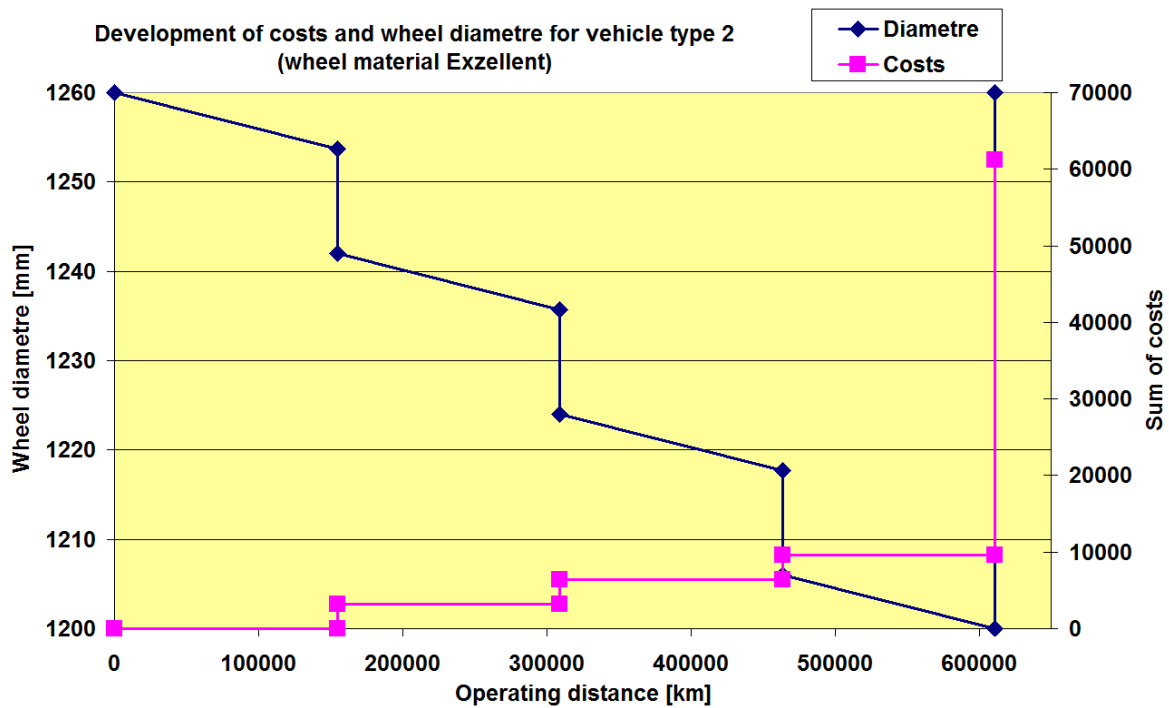


Figure 7.13: Durability diagram and costs for wheel material Exzellent

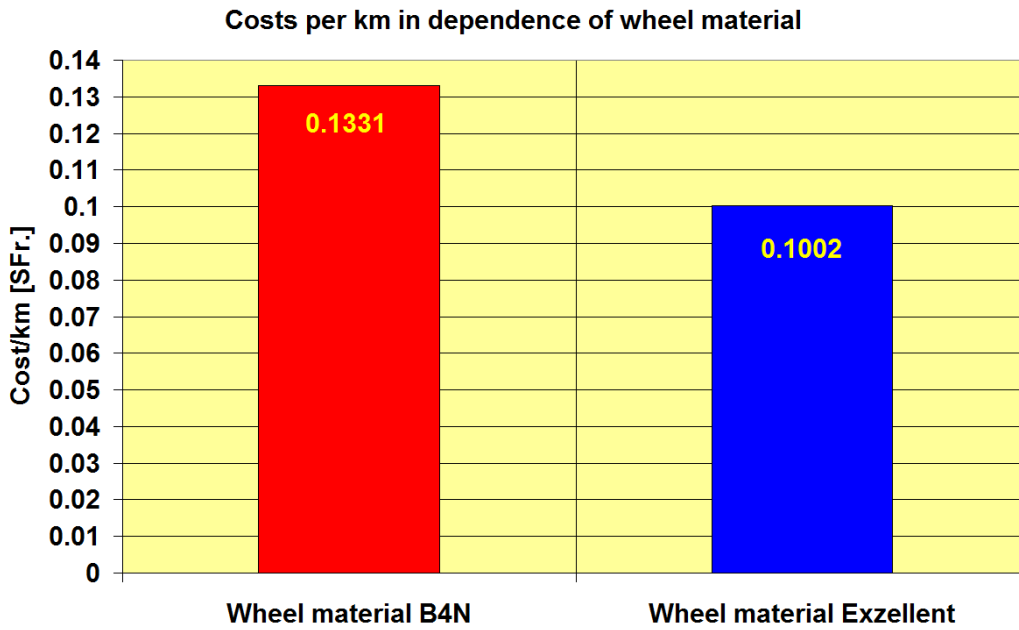


Figure 7.14: Cost per kilometre for the two different steel qualities

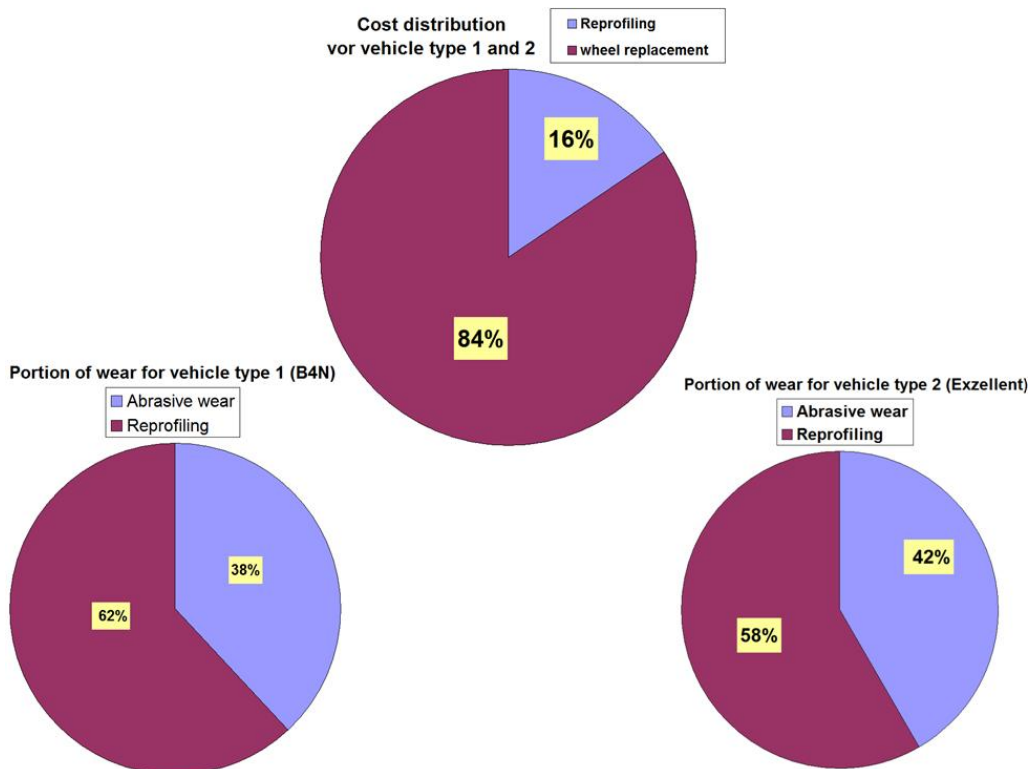


Figure 7.15: Cost distributions and portion of wear and portion of reprofiling

7.4 CONCLUSIONS

The calculations of the LCC at the wheelsets are based on the mileage-dependent removal of material due to wear on the wheels. Diameter reduction can happen on the one hand by removal in operation (wear) and on the other hand by the reprofiling. There are laws deriving from the mechanisms in the contact wheel/rail for both types of diameter reduction but unfortunately no information on OOR level development is available yet.

The vehicles considered here are type Re420 locomotives. The Re420 has two-axle trucks with an axle load of 20 tons. The horizontal connections of the wheelsets to the bogie frame are stiff. The dominant damage to the wheel treads are polygon formation and rolling contact fatigue. Dominating wear occurs on the wheel treads (flange wear is marginally). This type of wear can be represented as a linear function of the mileage. If this wear tends to propagate OOR on the wheels (polygons), it is crucial for reprofiling actions. If this is not the case, the reprofiling occurs due to RCF. A prediction of reprofiling intervals for RCF damages can be established on behalf of a Weibull distribution.

Durability charts show the performance of the wheels. In the present report mean values are shown for several investigated vehicles. The aim of this study was to determine the capability of different steel grades for the wheels. The steel commonly used in these vehicles is B4N (in the report referred to as type 1). The steel Excellent (called type 2) has a greater hardness than the B4N. The steel quality Excellent reduces the cost of the wheels per kilometre by 25%. 16% of the costs incurred for the reprofiling and 84% for the replacement of the wheelsets. Around 40% of the available rim thickness is removed by wear and 60% when reprofiling.

It turns out that even

- slightly smaller diameter reduction in the reprofiling
- higher wear resistance in service,
- somewhat more prolonged reprofiling intervals

have a significant cost saving. Due to steel grades greater hardness, the two indicators of wear and RCF can be positively influenced. Since the cost of the reprofiling are significantly lower than those for the wheel replacement, it should be examined whether the total cost can be significantly reduced by more frequent reprofiling.

An example for more frequent reprofiling with lower LCC for one specific train type was presented in deliverable D2.7 [4]. Unfortunately no information was available on OOR levels to see the influence on vibration mitigation.

8. FINAL CONCLUSIONS

It has been demonstrated that the wheel out-of-roundness has a significant influence on the vibration. It could be observed for the test train measurements both in Dottikon and in Brunnen that a reduction of the wheel irregularities with the amount of X dB by removing wheel out-of-roundness by maintenance roughly reduces the ground vibration with around an amount of X dB. This can be seen in the test train measurements of vibration and wheel out-of-roundness using locomotives of types Re420: both locomotives show differences of up to 20 dB between newly maintained and worn wheels. Dynamic force measurements also show similar amplitude differences.

In addition, the comparison of older OOR measurements with actual vibration measurements of the long term measurement campaign in Brunnen show similar amplitudes in some frequency bands. The vibration level scattering (95%-median value) for different vehicle types shows potential for improvement by maintenance. The insertion loss for some of the Re420 freight locomotives could reach values up to 12 dB. For Intercity trains, which are maintained more regularly to reduce structure borne noise in the vehicle, the potential for vibration reduction is low. The vibration spread for CARGO wagons is similar to the Locomotive Re420 and indicates potential for maintenance.

A statistical reanalysis of vibration measurements at different sites in Switzerland (Thun, Ligerz and Cadenazzo) indicate respectable potential for some of the vehicle types to reduce vibration excitation by maintenance. The freight wagons with bogie Y25 show for all 3 sites more than a factor of 2 for the maximum value divided by 95%-percentile value of the V_{rmsmax} -value. This indicates that a small percentage of freight wagons gives extremely high V_{rmsmax} vibration values and if these freight wagons could be maintained the maximum value of a freight train could decrease considerably by around a factor of 2 (6 dB).

The Swedish measurements carried out in the frame of work package 2.3 (deliverable D2.8) are analysed differently (whole train passage). Just little more scattering for freight than for Intercity trains is seen.

A LCC analysis is presented at the end of this document. The calculations of the LCC at the wheelsets are based on the mileage-dependent removal of material due to wear on the wheels. The vehicles considered here are type Re420 locomotives. The dominant damage to the wheel treads are polygon formation and rolling contact fatigue. The aim of the LCC study was to determine the capability of different steel grades for the wheels. The steel quality of the product Excellent, with greater hardness, reduces the cost of the wheels per kilometre by 25 %. 16 % of the costs incurred for the reprofiling and 84 % for the replacement of the wheelsets.

It turns out that even slightly smaller diameter reduction in the reprofiling due to higher wear resistance in service and therefore somewhat more prolonged reprofiling intervals have a significant cost saving. Due to steel grades with greater hardness, the two indicators of wear and rolling contact fatigue can be positively influenced. Since the cost of the reprofiling are significantly lower than those for the wheel replacement it should be examined whether the total cost can be significantly reduced by more frequent reprofiling. So it can be concluded that maintaining the wheels at a better OOR level does not necessarily lead to an increased LCC.

9. LITERATURE

- [1] Jens Nielsen, Roger Müller, Matthias Krüger, Thomas Lölgen, Pablo Mora, Pau Gratacos, Classification of wheel out-of-roundness conditions with respect to vibration emission, RIVAS (SCP0-GA-2010-265754), Deliverable 2.2, August 2012.
- [2] Jens Nielsen et al: RIVAS WP5 Deliverable D5.4: Train Induced Ground Vibration – Optimised Rolling Stock Mitigation Measures and their Parameters, 26.2.2013.
- [3] Brice Nelain, Philipp Huber, Adam Mirza, Mike Oppel, Roger Müller: Field test measurement report – the influence from vehicle design on the generation of ground-borne vibration, RIVAS (SCP0-GA-2010-265754), Deliverable 5.6, October 2013.
- [4] Roger Müller, Pau Gratacos, Pablo Mora, Jens Nielsen, Joseph Feng, Steven Cervello: Definition of wheel maintenance measures for reducing ground vibration, RIVAS (SCP0-GA-2010-265754), Deliverable 2.7, October 2013.
- [5] Pau Gratacos, Pablo Mora: Classification of Wheel Out-of-Roundness Conditions with Respect to Wheel OOR Database. RIVAS (SCP0-GA-2010-265754), Deliverable 2.4, February 2013.
- [6] Joseph Feng, Jens Nielsen, Bert Stallaert, Eric Berggren, Lise Pesqueux: Validation of track maintenance measures, RIVAS (SCP0-GA-2010-265754) Deliverable 2.8, December 2013.
- [7] Roland Müller: Estimation of Life Cycle Costs LCC, Gleislauftechnikmüller, Technical Report 07/01/12, December 2012.
- [8] SBB_P-OP-RM-FT-TM: Betriebsversuche Radreifenwerkstoffe Re 420 / Re 620, Interim report, March 2010.
- [9] Roland Müller: State of the art OOR and wheel/rail mechanisms, Gleislauftechnikmüller, Technical Report 07/01/12, December 2012.
- [10] M. Isida, M. Akama, K. Kashiwaya and A. Kapoor: The current status of theory and practice on rail integrity in Japanese railways - rolling contact fatigue and corrugation. Fatigue and fracture of Engineering Materials, V26,N010,2003, pp. 909-919
- [11] Adam Bevan, Paul Molyneux-Berry, Bridget Eickhoff, Mark Burstow: Development and Validation of a Wheel Wear and Rolling Contact Fatigue Model, University of Huddersfield Repository.
- [12] Paul Molyneux-Berry, Adam Bevan: Wheel surface damage: Relating the position of angle and forces to the observed damage patterns, University of Huddersfield Repository.
- [13] Mikael Palo, Jing Lin, Per Olof Larsson Kraik: Maintenance Performance Improvement for Rolling Stock Wheels, Chemical Engineering Transaction, Vol. 33, 2013
- [14] BSSR: Cost effective turning of flange worn wheel profiles, project number T641.
- [15] M. C. Burstow: Whole life Rail Model application and development of RSSB – Continued development of an RCF damage parameter. Rail safety and Standards Board London (2004)

ANNEX A MAINTENANCE PROCESS

Figure A1 shows the overall methods to detect and monitor wheel wear and wheel fatigue. One is visual inspection of the wheels at the railway yard or in the near service workshops. Another is the use of wayside monitoring stations to detect wheel tread faults (impact loads). A third option is during general vehicle maintenance in workshops. Wheel maintenance decision criteria are stricter and more rigid at vehicle workshop than in the railway yard. If a vehicle with bad wheels is at the workshop, the wheels can be maintained before they reach their maintenance limit (opportunity based maintenance actions). There are a number of fault parameters that determine the proper maintenance action for the wheels before it is put back into service.

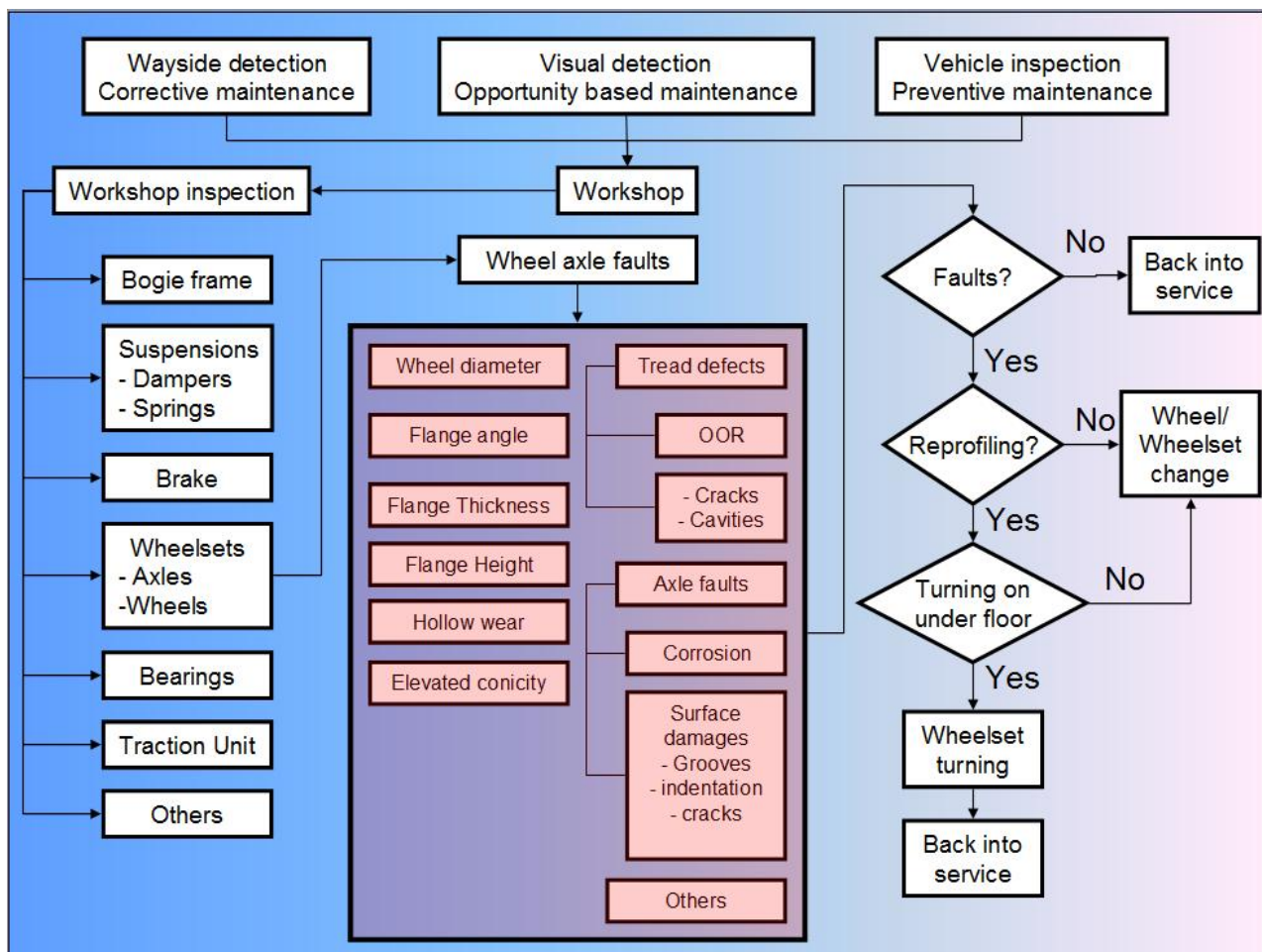


Figure A1: Inspection and maintenance process [13]

Figure A1 shows the overall maintenance process. The work order for a vehicle to appear at the workshop can come from different sources: safety alarms, driver's reports, visual inspection or pre-determined distances. Figure A2 looks specifically at wheels, illustrating what happens to a wheel with a damage or geometry fault/failure at the beginning of the maintenance process. A faulty wheel is detected either visually, using wayside detection systems, or manually using hand-held monitoring equipment. From here, a work order is generated and the wheel goes to the next stage. Either of these stages can have a fault that is not detected. These non-detected faults represent a certain safety or risk cost. The risk/safety factor or cost shown in Figure A2 refers to when a wheel has a fault that

is not detected. In that case, the wheel will run to failure before it is caught in another detection cycle.

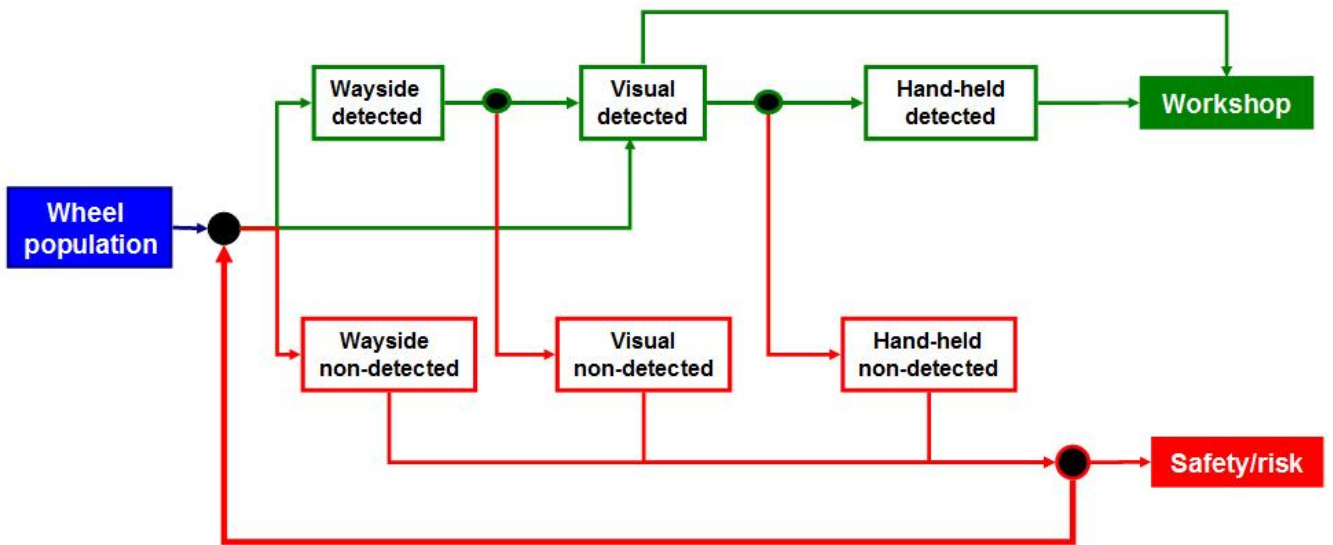


Figure A2: Process of wheel detection

ANNEX B WHEEL TREAD DAMAGE GUIDE

The wheel tread damage guide aims to assist fleet engineers in optimising the life of their wheelsets and minimising the associated costs. It also provides descriptions and photographs that will be useful to wheel lathe operators when identifying unfamiliar damage types. A guide includes:

- Description of different forms of damage observed on the wheel treads (including illustrations, causes and mechanisms).
- Information on the level of data that should be captured to improve the understanding of wheel damage.
- How this data can be analysed to identify key issues, which dominate wheel life.
- Guidance on selecting the most appropriate course of action for reducing wheel tread damage.

The damage types, which should be included in the guide, are summarized in Figure B1. The different damages can be attributed to mechanisms causing them. If the maintenance is to be optimized, so the decisive reasons for reprofiling must be known and their underlying mechanisms need to be understood.

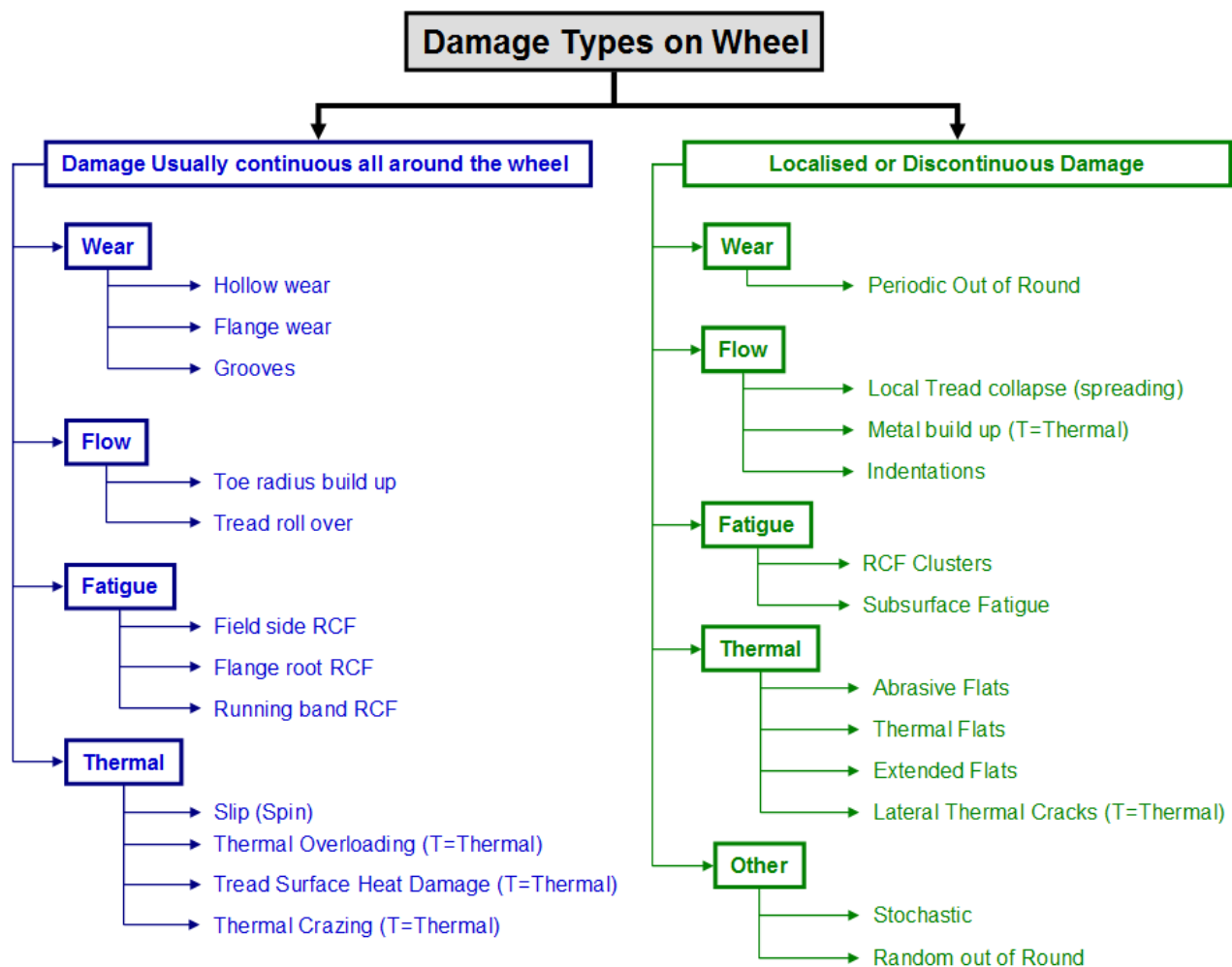


Figure B1: Damage types on wheels

Also the methodology for improving and understanding the wheel damage on a fleet has to be detailed. This is summarized in Figure B2. The methodology consists of a number of levels (1 to 4). Each level in Figure B2 provides the foundations for the subsequent levels and therefore to get the most out of the upper levels, robust methods to complete the lower levels must first be in place.

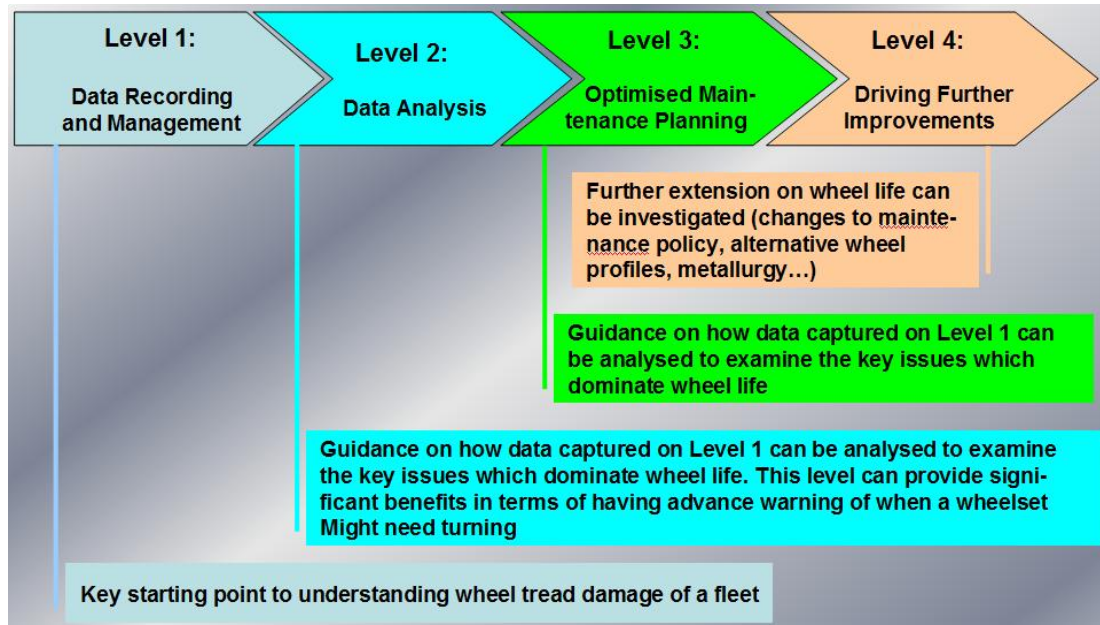


Figure B2: Management and optimisation of wheelset life

Management and optimisation can be based on case studies, which demonstrate

- How simple data analysis can be used to determine the issues which drive wheelset life;
- The use of condition monitoring to detect damage and trigger early intervention;
- Optimisation of a preventive wheel turning interval;
- Use of wheel lathe data to compare bogie types and support a business case for modifications;
- The influence of wheel material and wheel profile on wheel turning intervals.

As illustrated in Figure B1 there can be different criteria for determinant faults causing reprofiling. In dependence of determinant faults, different mitigation methods for upgrading maintenance costs can be applied. There is a difference if the determinant fault is minimum flange thickness, maximum flange height or rolling contact fatigue.

In [14] investigation focussed on addressing the following two key issues for wheelsets with predominant wheel flange wear:

- Is there any benefit on more frequent re-profiling of flange worn profiles?
- Is it feasible to adopt wheel profiles with a thinner flange and, if so, is there any benefit in doing so?

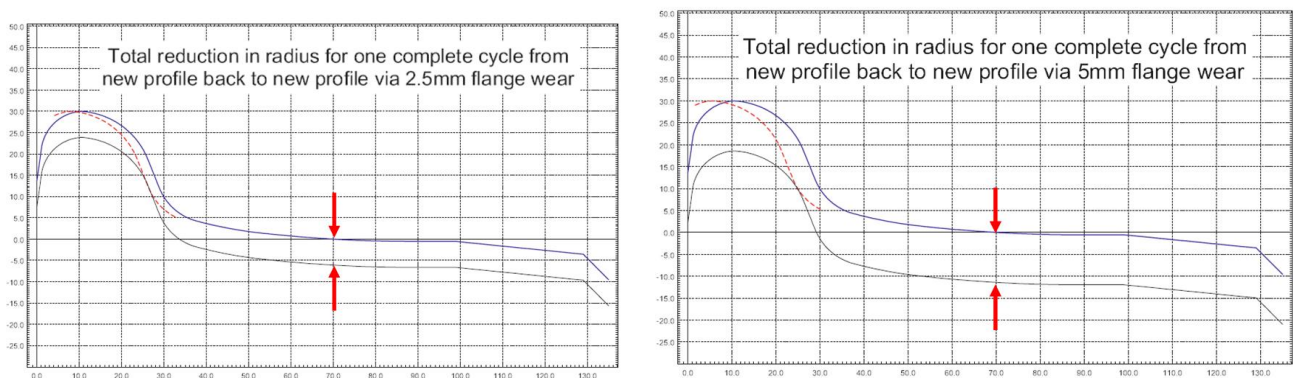


Figure B3: Total reduction of wheel radius for one complete cycle in dependence of flange wear

Relationship between flange wear and total reduction in radius for one complete cycle from new profile back to new profile (Dashed line indicates the trend if the relationship were linear)

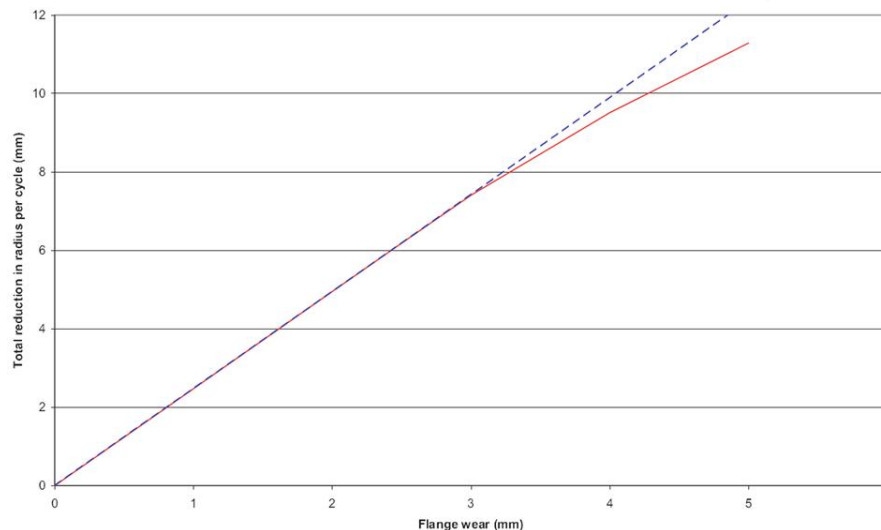


Figure B4: Relationship between flange wear and radius reduction to achieve new profile

Figure B3 shows two different worn wheel profiles both suffering from flange wear. Figure B4 shows the relationship between flange wear and radius reduction. It can be seen that a flange wear of 1 mm affords a radius reduction of 2.5 mm. This is a key relationship with the following implications:

- Where flange wear is the limiting factor there is no advantage in more frequent reprofiling.
- Removing a greater amount of flange wear takes (proportionally) less off the wheel radius and is therefore preferred.
- Reprofileing back to the new profile should be delayed for as long as possible.

The standard mitigation for the control of flange wear, detailed in the literature and used by other administrations, is effective lubrication. It is therefore recommended that a cost benefit analysis is undertaken to quantify the financial consequences of flange wear against the costs of a lubrication regime, either track or train mounted, or both.

In other cases, RCF damage is observed to form much more rapidly on wheels, which are reaching the end of their life, as shown in Figure B5. The red line shows the wheel-diameter to remove for RIVAS_SBB_WP2_D2_9_V5

restoring the profile (for example due to flange wear). After a certain mileage, the determinant fault changes from flange wear to RCF.

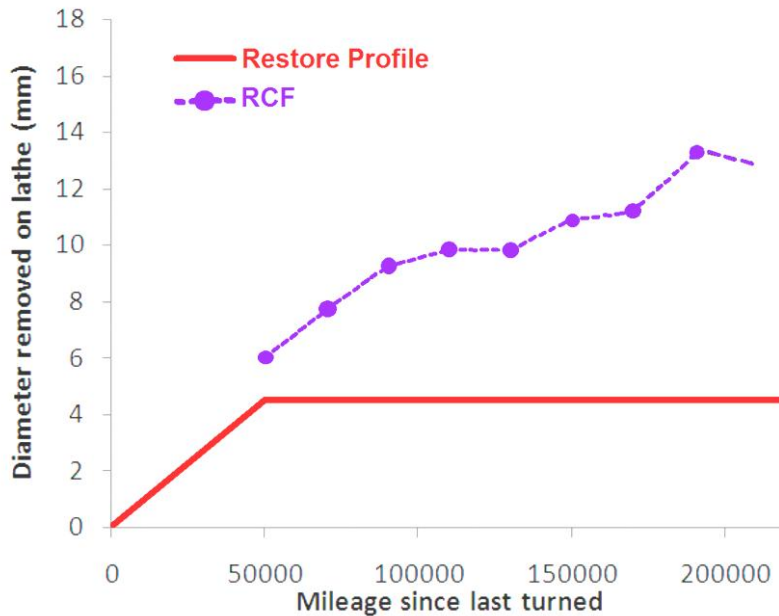


Figure B5: Diameter reduction in function of determinant faults

The energy expended in the wheel/rail contact expressed as T_γ has also been used to express RCF damage. Wear and RCF are two separate phenomena that nonetheless have some influence on one another. Burstow [15] thus developed a weighted function taking into account the summation of these two phenomena, one for wear and the other one for fatigue. Figure B6 shows a graph of the weighted T_γ function with the T_γ value on the abscissa and the resulting damage function on the ordinate. Three stages can be observed with RCF only at low energy dissipation between 15 and 75N, a zone of combined wear and RCF for values in between 65 and 175N and above that the wear regime becomes predominant by removing any RCF crack before they can become significant. This method has been used extensively in the UK and effort were spent in developing it as part of an asset and risk management tool.

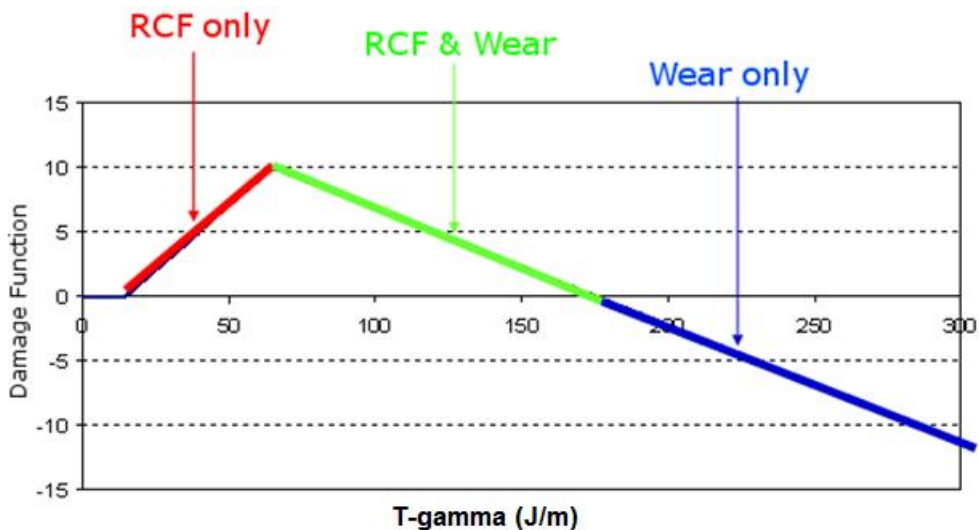


Figure B6: Weighted T-gamma function